Global Hunger and Climate Change Adaptation through International Trade

Charlotte Janssens, Petr Havlik, Tamas Krisztin, Justin Baker, Hasegawa Tomoko, Nicole Van Lipzig, Miet Maertens

Selected paper prepared for presentation at the 2019 Summer Symposium: Trading for Good – Agricultural Trade in the Context of Climate Change Adaptation and Mitigation: Synergies, Obstacles and Possible Solutions, co-organized by the International Agricultural Trade Research Consortium (IATRC) and the European Commission Joint Research Center (EU-JRC), June 23-25, 2019 in Seville, Spain.

Global hunger and climate change adaptation through international trade

Janssens Charlotte[1,2], Havlik Petr[1], Krisztin Tamas[1], Baker Justin[3], Tomoko Hasegawa[1,4], Nicole Van Lipzig[2], Miet Maertens[2]

[1] International Institute for Applied System Analysis (IIASA), Schlossplatz 1, A-2361 Laxenburg, Austria
[2] University of Leuven (KU Leuven), Department of Earth and Environmental Sciences, Celestijnenlaan 200E, Heverlee, Belgium
[3] RTI International, 3040 East Cornwallis Road, Durham, NC 27709-2194, United States of America
[4] Center for Social and Environmental Systems Research, National Institute for Environmental Studies (NIES), National Institute for Environmental Studies, 16–2 Onogawa, Tsukuba, Ibaraki 305–8506, Japan

Approximately 11% of the 2017 world population or 821 million people had insufficient dietary energy for a healthy and active life (FAO et al. 2018). Undernourishment is increasing since 2014 and is most prevalent in Sub-Saharan Africa (23.2% of the population), the Caribbean (16.5% of the population) and Southern Asia (14.8% of the population) (FAO et al. 2018). Reaching UN Sustainable Development Goal 2 to end global hunger by 2030 is jeopardized by climate change (Hoegh-Guldberg et al. 2018). Climate change is projected to raise agricultural prices (Nelson et al. 2014) and to expose in total an additional 77 million people to risk of hunger by 2050 (IFPRI, 2019). Policy strategies to safeguard food security under climate change focus on technical innovations such as new crop varieties and climate-smart farming practices, and intra- and international reallocation of agricultural production (Hertel 2018; Nelson et al. 2014).

The latter includes a focus on international trade as an important adaptation mechanism (Huang, von Lampe, and van Tongeren 2011; Brown et al. 2017). Trade links food deficit and surplus countries and raises countries' food consumption possibility through specialization in the production of crops for which countries have a comparative advantage. Climate change affects regions and crops differently (Rosenzweig et al. 2014), possibly causing shifts in regional comparative advantages and raising potential for new trade patterns. Studies evaluating the role of trade in agricultural adaptation find that restricting trade exacerbates the negative impact of climate change on agricultural welfare, while liberalizing trade attains the opposite effect (Stevanović et al. 2016; Wiebe et al. 2015; Gouel and Laborde 2018; Costinot, Donaldson, and Smith 2016; Baldos and Hertel 2015; Cui et al. 2018). However, with the exception of Cui et al. (2018), these studies do not assess whether the findings result solely from a pure trade effect – in that case trade integration has the same effect with or without climate change – or whether a real adaptation effect is involved – meaning that the impact of trade integration becomes larger under climate change.

We focus on global hunger projections towards 2050, and analyze how climate change and trade liberalization and facilitation scenarios interact in their impact on hunger. We use an established economic (GLOBIOM) and crop (EPIC) modeling approach to investigate climate change impacts on the agricultural sector (Mosnier et al. 2014; Leclère et al. 2014; Baker et al. 2018; Havlík et al. 2015). GLOBIOM is a partial equilibrium model with a bilateral trade specification, that allows for detailed trade cost analysis, and models the emergence of new trade patterns in response to climate change (as opposed to Armington-based models). We analyze a set of 50 integrated trade and climate change scenarios that capture variability in regional trade barriers and in climate projections originating from different models,

emissions scenarios and CO_2 fertilization effects. This approach makes three innovations to the literature. Building on our large set of scenarios we estimate the adaptation effect of trade in a more robust way using a regression framework, we assess both tariff and non-tariff type trade barriers, and we include trade effects at the intensive and extensive margin.

The adaptive effect of international trade for global hunger

Building on the approach of Baker et al. (2018), this paper uses ten climate change and five trade scenarios, and analyzes hunger effects at the global and regional level. Four representative concentration pathways (RCPs, 2.6 Wm^{-2} scenario, 4.5 Wm^{-2} scenario, 6 Wm^{-2} scenario and 8.5 Wm^{-2} scenario) are projected by the HadGEM2-ES general circulation model (GCM) with CO_2 fertilization effects, and, for RCP8.5, also without CO_2 fertilization effects. RCP8.5 is implemented with 4 alternative GCMs (GFDL-ESM2M, NorESM1-M, IPSL-CM5A-LR, and MIROC-ESM-CHEM). Crop yields that are projected by the EPIC crop model under the nine RCP x CO_2 x GCM combinations are compared to projections without climate change impacts (NoCC). In the *Baseline trade* scenario trade barriers are kept constant at 2000 level. The *Fixed imports* scenario prevents agricultural imports to be larger than in the NoCC scenario. In the *Facilitation* scenario, barriers that limit the expansion of trade (e.g. transaction costs, infrastructure costs) are set close to zero, as in Baker et al. (2018). In the *Tariff elimination* scenario agricultural tariffs are progressively phased out between 2020 and 2050, i.e. -25% in 2020, -50% in 2030, -75% in 2040 and -100% in 2050. Lastly, the *Facilitation + Tariff elimination* scenario combines the previous two. Socioeconomic developments are modelled according to the second Shared Socio-Economic Pathway (SSP2), where global population reaches 9.2 billion by 2050 and regional income grows according to historical trends (Fricko et al. 2017). The scenario design is discussed in further detail in Methods.

Through adjustments in trade, supply and demand induced by the different climate and trade scenarios, the 2050 global population at risk of hunger deviates substantially from the SSP2 baseline projection (Figure 1, Supplementary Table 1 and 2). First, without changes in trade barriers, projections across RCP8.5 scenarios range from a reduction of 3 million to an increase of 48 million hungry people compared to the baseline (-2% to +29%), depending on the GCM and CO_2 fertilization effect. With *Fixed imports*, hunger exacerbates across all RCP8.5 scenarios, with in the most extreme case an additional 89 million hungry people compared to the baseline (+54%). This means that some regions importantly depend on agricultural imports to limit the impact of climate change on hunger. In the *Baseline trade* scenario, the total agricultural trade volume increases 2% to 14% across RCP8.5 scenarios through an expansion at the intensive as well as extensive margin (new flows representing 1% – 2.5% of the total trade volume) (Supplementary Table 1). By preventing endogenous market responses to climate change the *Fixed imports* scenario leads to a lower global crop production efficiency (-1% to -3%), a lower total crop calorie production (-1% to -3%), higher agricultural prices (+2% to +10%), and lower global food availability (-12 to -40 kcal/cap/day) across RCP8.5 scenarios compared to the *Baseline trade* scenario (Supplementary Table 2). On average, *Fixed imports* increases the hunger effect of RCP8.5 scenarios by 144%, which is larger than the impact of trade restriction found by Wiebe et al. (2015) on food price effects (63%) and by Gouel and Laborde (2018) on agricultural welfare effects (76%).

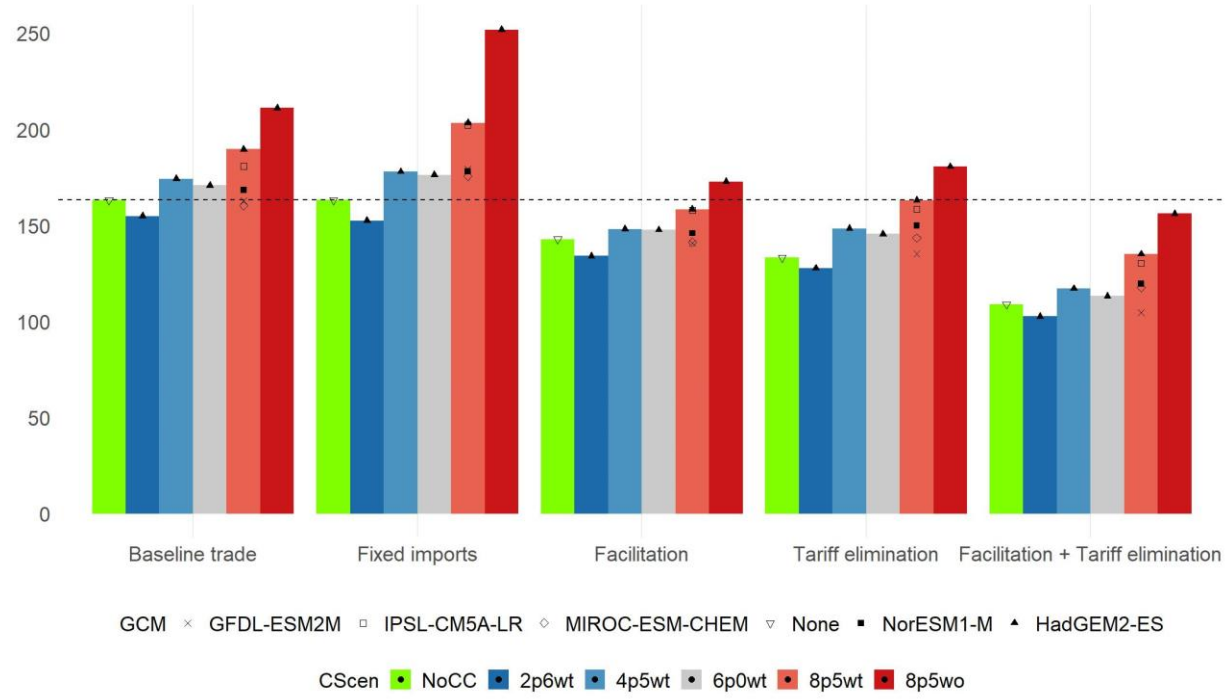

Figure 1 | Global population at risk of hunger (million) in 2050 across climate change and trade scenarios. wt: with CO_2 fertilization effect, wo: without CO_2 fertilization effect. The black dotted horizontal line indicates the population at risk of hunger in the SSP2 baseline (163 million).

Second, the *Facilitation* and *Tariff elimination* scenarios both reduce the risk of hunger from climate change, but it is only in the *Facilitation + Tariff elimination* scenario that the impact of the most negative climate change scenario is fully compensated. Trade liberalization and facilitation reduces hunger by enhancing climate-induced trade adjustments – total agricultural trade triples to quadruples across RCP8.5 scenarios with more important adjustments at the extensive margin (new trade flows representing 5 to 8% of total trade volume) – and by increasing the efficiency of agricultural production under climate change (Supplementary Table 1 and 2). Either trade liberalization or trade facilitation suffices to compensate the impact on hunger under intermediate climate change scenarios (RCP4.5wt – RCP6wt). In RCP2.6wt the population at risk of hunger is consistently lower than the SSP2 baseline because crop yields in many regions increase or remain unaffected in this scenario (Supplementary Figure 1). The hunger effect under the most extreme climate change scenario is reduced by 79% under *Facilitation*, 63% under *Tariff elimination* and 114% under *Facilitation + Tariff elimination*. These are larger than the 44% lower hunger effect under market integration in Baldos and Hertel (2015) or the 46% lower price effect under trade liberalization in Wiebe et al. (2015).

To analyze how climate change and trade scenarios interact in their impact on hunger, and thus to reveal the adaptation effect of trade, we regress hunger outcomes from GLOBIOM on crop yield shocks projected by EPIC and average trade costs in regional level linear regression models (Table 1). We interpret these results for a 6% reduction in crop yield and a 29% reduction in trade costs, which corresponds to the average impacts of climate change scenarios and trade policy scenarios respectively. Regression results (Table 1) reveal that a 6% reduction in crop yields within a region leads on average to a reduction in food availability of 11 kcal/cap/day (95% confidence interval (CI), 13 – 9 kcal/cap/day) and an additional 0.65 million people at risk of hunger (CI, 0.29 – 1 million). For a 29% decrease in trade costs, we project that

average food availability within a region increases 11 kcal/cap/day (CI, 9 – 13 kcal/cap/day) and that there are 1.53 million fewer people undernourished (CI, 1.89 – 1.18 million). Regional differences matter and are discussed in the next section. We find a significant negative interaction effect between trade costs and climate-induced crop yield change. This means for example that the average hunger impact of a 6% climate-induced reduction in crop yields is more than halved (from an additional 0.65 million to an additional 0.26 million hungry people) with a 29% reduction in trade costs. The adaptation effect of reducing trade costs by 29% is -0.39 million hungry people. When considering also the direct positive effect of reducing trade costs, the impact of a 6% reduction in crop yield is already completely compensated by a 11% reduction in trade costs – the negative hunger effect of a 6% reduction in crop yields (+0.65 million) is offset by the sum of the direct effect (-0.52 million) and the adaptation effect (-0.13 million) of reducing trade costs by 11%. These results imply that trade costs importantly determine how climate change affects hunger (or that climate change alters the relation between agricultural trade and global hunger) and point to a global climate change adaptation potential of reducing trade costs through trade liberalization and facilitation.

Table 1 | Results from OLS estimation of the impact of crop yields, trade costs and their interaction on population at risk of hunger and food availability. Observations are GLOBIOM output for each region under the 5 different trade scenarios and 10 different climate change scenarios in 2050. The regression models are described in the Methods.

	Population at risk of hunger (million)	Food availability (kcal/cap/day)
Crop yield	-11.497 ***	191.791 ***
(% change)	(3.213)	(18.021)
Trade cost	4.528 ***	-32.517 ***
	(0.538)	(3.596)
Crop yield (% change) x	-20.149 ***	65.838 **
Trade cost	(6.685)	(28.481)

Significance levels: *p<0.1; **p<0.05; ***p<0.01. Regional fixed effects included. Two outliers are removed, [EUR, T1, 8p5wo] and [CSI, T1, 8p5wo]. Heteroskedastic robust standard errors in brackets. N = 548. Adjusted R squared is 0.916 for hunger regression and 0.977 for food availability regression.

Regional perspective on trade's adaptation potential

The hunger outcomes of different climate and trade scenarios differ substantially among regions (Figure 2). South Asia (SAS) and Sub-Saharan Africa (SSA) are most severely affected by climate change and experience the largest hunger-increasing effect from import restrictions. Across RCP8.5 scenarios, projections for the *Baseline trade* scenario range from a marginal reduction to a large increase in population at risk of hunger in SAS and SSA (-2% to +75% and -1% to +35% compared to the baseline, respectively). Across these scenarios, SAS and SSA become larger net agricultural importers (net imports increase by 23 to 137% in SAS and by 7 to 40% in SSA), increasing imports from regions with the highest crop yields across RCP8.5 scenarios, LAC, EUR and EAS (Supplementary Figure 1). Intra-regional trade increases by 14% to 57% in SSA, but varies across RCP8.5 scenarios in SAS (+10% to -36%). With *Fixed imports* an additional 7 to 51 million people are at risk of hunger in SAS, while in SSA the impact ranges from a reduction of 0.83 million to an increase of 27 million. Preventing trade adjustments to climate change increases agricultural prices and lowers food availability. Consistent with the global picture,

Facilitation + Tariff elimination reduces agricultural prices, increases food availability, and reduces hunger in SAS and SSA across all RCP8.5 scenarios. SAS faces higher agricultural tariffs in 2000 than SSA leading to larger absolute changes in terms of prices, food consumption and hunger from tariff elimination. Other regions experience much smaller hunger effects of climate change and trade scenarios. This is in line with other studies showing that South Asia and Sub-Saharan Africa are most vulnerable to climate change and would benefit most from trade integration (Gouel and Laborde 2018; Baldos and Hertel 2015).

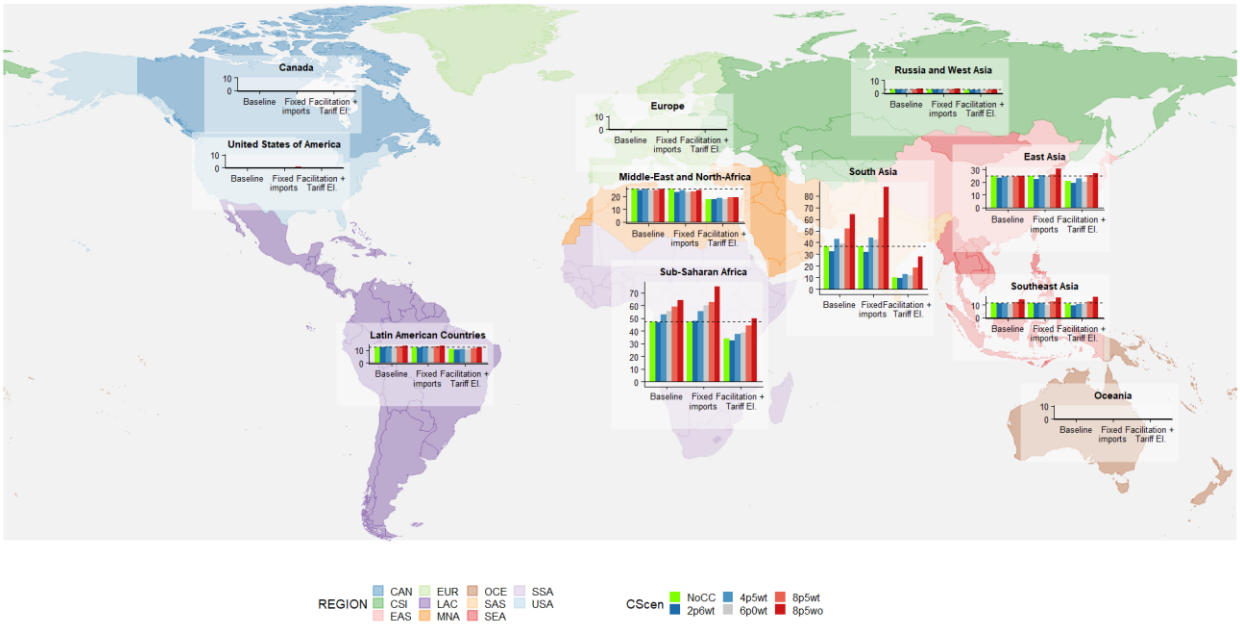

Figure 2 | Population at risk of hunger in 2050 under different climate change and trade scenarios in each region (million). Regions are United States of America (USA), Russia and West Asia (CSI), East Asia (EAS), Southeast Asia (SEA), South Asia (SAS), Middle-East and North-Africa (MNA), Sub-Saharan Africa (SSA), Latin American Countries (LAC), Oceania (OCE), Canada (CAN) and Europe (EUR). The population at risk of hunger is zero in each climate change and trade scenario in CAN and EUR. The black dotted horizontal line indicates the population at risk of hunger in the SSP2 baseline.

To reveal regional differences in how climate change and trade scenarios interact in their impact on hunger, we add regional interaction effects in the regressions presented in Table 1 (Supplementary Table 3). In most regions, climate-induced decreases in crop yields reduce food availability and increase hunger while reduced trade costs have the opposite effects, with the largest impacts in low-income regions (SSA and SAS), followed by middle-income regions (EAS, MNA, CSI and LAC). In USA and OCE reduced trade costs slightly reduce food availability while hardly affecting hunger. Reduced food availability translates into either large, small or insignificant effects on hunger, depending on regional income levels. As described in Hasegawa et al. (2015; 2018), at similar per capita food availability levels, risk of hunger is higher in low-income countries because of an inverse relationship between per capita income and inequality in domestic food distribution. The latter relates to poor infrastructure and remoteness which limit local markets in distributing food equally (Brown et al. 2017).

The hunger effect from the interaction between trade costs and climate-induced yield changes, i.e. the adaptation effect of reducing trade costs, is large and negative only for SSA and SAS (Supplementary Table 3). A 6% reduction in crop yields increases hunger in SAS on average with 4.47 million people and is offset by a 29% reduction in trade costs through a direct effect (-3.86 million) and adaptation effect (-0.61

million). In SSA, a 6% reduction in crop yields increases hunger on average with 5.24 million people and is compensated by a 26% reduction in trade costs through a direct effect (-4.29 million) and adaptation effect (-0.96 million). Figure 3 plots the predicted hunger-yield relationship in SAS and SSA for different levels of international trade costs (Supplementary Figure 2 for all regions). This visual illustrates the direct effect of trade costs (a downward shift of the curve for lower trade costs) and the adaptation effect of trade costs (a flatter slope for lower trade costs). The importance of the trade adaptation effect increases the more negative climate-induced crop yield change. For example, in SSA the estimated hunger effect of the average crop yield change in the most extreme climate change scenario (RCP8.5wo, -21% reduction in crop yield) is an additional 19.2 million people undernourished and is compensated by a 50% trade cost reduction through a direct effect of -10.5 million and adaptation effect of -8.7 million people hungry. Especially in the poorest regions (SAS and SSA) climate-induced crop yield changes increase hunger and lower trade costs through trade liberalization and investments in trade infrastructure reduce hunger, directly and indirectly by lowering the sensitivity of hunger to climate change.

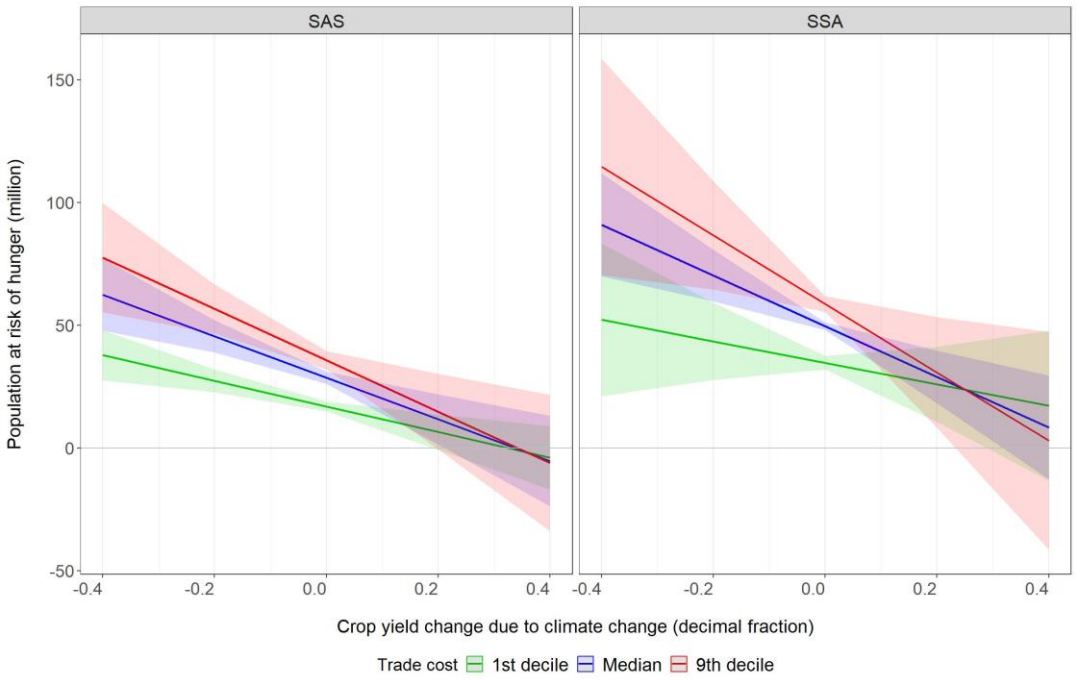

Figure 3 | Plot of the fitted linear response of population at risk of hunger (million) to climate-induced crop yield change in SAS and SSA for different values of trade costs (1st decile, median, 9th decile). Shaded areas indicate prediction intervals. Prediction based on an OLS estimation of a regional level linear regression of the impact of crop yield change, trade costs and their interaction on population at risk of hunger. Regression results are shown in Supplementary Table 3 and the regression model is described in Methods.

Inter-regional specialization

In Figure 4 we assess to what extent climate change shifts the pattern of comparative advantage of four key staple food crops (corn, wheat, soya and rice) across GCMs and RCPs. In line with Ricardo's theory, a region is regarded as having a comparative advantage when it specializes in a certain crop, such that its share of world production increases, when trade costs reduce. Under no climate change, USA has a comparative advantage in corn production, LAC in soya, and OCE and EUR in wheat (Figure 4a). Under

climate change, LAC and USA have a comparative advantage in corn production, SEA and EAS in rice, LAC in soya, and OCE, CSI, EUR and CAN in wheat (Figure 4b). Figure 4c compares regions' specialization in response to a trade cost reduction under climate change and no climate change. The small number of significant differences reveals that the overall pattern of comparative advantage of the four crops remains similar under climate change. While climate change affects the relative productivity and cost competitiveness of regions, it does not radically alter the relative position of each region for these crops (Supplementary Figure 3 and 4). Figures on crop shares in a region's total production, and on export shares in a region's crop production (Supplementary Figures 6 and 7) corroborate this. SAS and SSA increase total agricultural imports under climate change, indicating a low comparative advantage in overall agricultural production. Climate change increases particularly the import of those crops for which SAS and SSA already have a large net import in the baseline (soya in SAS, and rice and wheat in SSA, Supplementary Figure 8). These increased imports originate from major baseline producing regions, which maintain a comparative advantage under climate change (soya from LAC, wheat from EUR and rice from EAS and SEA, cfr. Figure 4b and Supplementary Figure 5). The impact of climate change on rice in SAS and corn in SSA, which are of critical importance in regional food production and consumption, is mixed. In the baseline, SAS is a large producer of rice with small net imports to satisfy its consumption (Supplementary Figure 5 and 8). Under intermediate climate change scenarios, SAS becomes a net rice exporter, while under RCP8.5 scenarios it becomes a larger net rice importer. This trend remains in the *Facilitation* scenario, while under *Tariff elimination* SAS becomes a larger net rice importer in each climate change scenario. SSA is large corn producer and a net exporter in the baseline (Supplementary Figure 5 and 8). Across all climate change scenarios, SSA maintains a surplus corn production and increases its net exports, increasing trade specifically to SAS and EAS. In the trade scenarios, most strongly under *Facilitation*, SSA further increases its net corn exports. Besides increasing exports to EAS and SAS, SSA also increases its intra-regional trade.

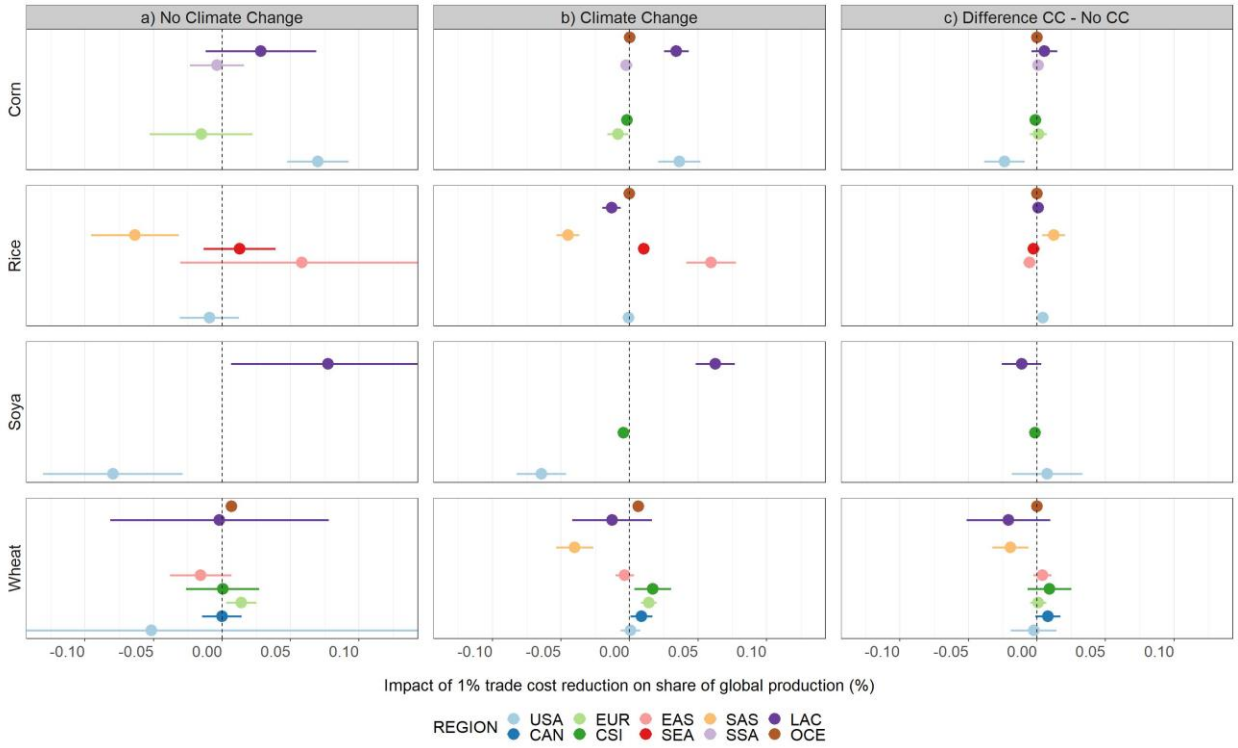

Figure 4 | Inter-regional specialization in corn, rice, soya and wheat in response to trade cost reduction in 2050 under a) constant climate, b) climate change, and c) the difference between climate change and no climate change. Each subplot presents the results of a crop-specific OLS estimation of a regional level linear regression model on the impact of export trade costs on share of global production. Each point shows the estimated impact of a 1% reduction in trade costs on exports for a particular crop and region on share of world production in percentage, with lines denoting the corresponding 95% confidence interval (heteroskedastic robust standard errors). For **a)** observations are taken from the constant climate change scenario and 4 trade scenarios (*Baseline trade, Facilitation, Tariff, Facilitation + Tariff*). Only regions are selected whose share of world production of the crop in the baseline is larger than 1%, and which have a surplus production of the crop in at least one of the three trade integration scenarios. 95% confidence interval of USA – wheat is [-0.24, 0.35]. N is 16 for corn, 16 for rice, 8 for soya, and 27 for wheat. For **b) and c)** observations are taken from the 9 climate change scenarios and 4 trade scenarios (*Baseline trade, Facilitation, Tariff, Facilitation + Tariff*) with exclusion of regions that have a deficit production in each trade and climate change scenario. N is 215 for corn, 216 for rice, 108 for soya and 263 for wheat. For **c)** the outcome variable is the difference in share of world production with the no climate change scenario. The regression models are described in the (Supplementary) Methods.

Existing literature suggests that trade acts as an adaptation mechanism because it facilitates responses to a climate-induced altered pattern of comparative advantage (e.g. Costinot et al 2016; Gouel and Laborde 2018). We provide quantitative evidence for a climate change adaptation effect of trade. Yet, changing comparative advantage in crops is not the main driver of this effect. Our results suggest that trade liberalization and facilitation creates the largest gain in food availability for regions with a deficit production and low yield for staple food crops, which are the regions that are most vulnerable to undernourishment due to low income endowments (Supplementary Figures 4, 9 – 12). This explains the high climate change adaptation effect on hunger of trade adjustments in SAS and SSA.

Discussion

International trade contributes importantly to climate change adaptation, especially in the poorest and most hunger-affected regions. Trade liberalization and facilitation can completely compensate the hunger-increasing effect of climate change, even in the worst climate change scenario. We find that under the worst climate change conditions, hunger is 107% lower with open trade than with restricted trade. Others focusing on agricultural GDP by 2100 come to more conservative estimates of 62.5% ((Stevanović et al. 2016)) and 81% (Gouel and Laborde, 2018). We quantify the climate change adaptation effect of trade, showing that it becomes larger the more negative the climate-induced yield impact. By expanding explorative scenario analyses, accounting for how climate change and trade interact in their impact on hunger, and allowing for trade adjustments at the intensive and extensive margin, we demonstrate a more substantial role for trade in climate change adaptation. Despite these important methodological innovations there are limitations to this study, which paves the way for further research. With a focus on food availability, long term trends and climate change adaptation, we do not account for distributional issues of food and nutrition security, short term shocks and extreme weather events, and potential adverse climate mitigation effects of trade.

Our results imply an enormous potential to use trade instruments to mitigate adverse hunger effects of climate change and thereby endorse the importance of the Doha Round of trade negotiations. Climate change alters the trade food security nexus, calling for a better integration of a climate policy agenda within the Doha Development Agenda. The innovative insight from this paper that the benefits of trade liberalization increase substantially with more severe climate change, implies that contemplating the climate change adaptation potential of trade in negotiations might even facilitate resuming the Doha agenda. We need to stress that compensating for climate-induced increases in hunger requires both trade liberalization by relaxing import tariffs and facilitation through investments in trade infrastructure. Particularly for SSA and SAS trade policies should be an important element in climate adaptation strategies, as these regions are not only most vulnerable to climate-induced hunger but also have the largest potential to compensate this through further trade liberalization and facilitation.

Method

Modelling framework We use the Global Biosphere Management Model (GLOBIOM) for our analysis. GLOBIOM is a recursive dynamic, spatially explicit, economic partial equilibrium model of the agriculture, forestry and bioenergy sector. Starting in 2000, the model computes a market equilibrium in 10 year time steps until 2050 by maximizing welfare (the sum of consumer and producer surplus) subject to technological, resource and political constraints. On the demand side, a representative consumer for each one of the 30 economic regions optimizes consumption in response to product prices and income. For this paper, we mainly present the model results aggregated to 11 world regions: United States of America (USA), Canada (CAN), Europe (EUR), Oceania (OCE), Southeast Asia (SEA), South Asia (SAS), Sub-Saharan Africa (SSA), Middle-East and North-Africa (MNA), East Asia (EAS), CSI (Russia and West Asia) and Latin American Countries (LAC). In the aggregation of trade flows and trade costs between the 30 economic regions, a distinction is made between extra-regional (among world regions) and intra-regional trade (within one world region). GLOBIOM is a bottom-up model building on a high spatial grid-level resolution on the supply side. Land is disaggregated into Simulation Units, clusters of 5 arcmin pixels which are aggregated based on the same altitude, slope and soil class, 30 arcmin pixel and country boundaries. GLOBIOM's crop production sector includes 18 major crops (barley, beans, cassava, chickpeas, corn, cotton, groundnut, millet, palm oil, potato, rapeseed, rice, soybean, sorghum, sugarcane, sunflower, sweet potato, wheat) under 4 management systems (irrigated – high input, rainfed – high input, rainfed – low input and subsistence). Crop production parameters are based on the detailed biophysical crop model EPIC. Additional biophysical models are used to represent the livestock [RUMINANT - (Herrero et al. 2013)] and forestry [G4M – (Forsell et al. 2016)] sectors. Further information regarding the model structure and parameters is documented in (Havlík et al. 2011; Havlik et al. 2014).

Crop yields adjust endogenously in the model by changing the management system or location of production, and exogenously according to long-term technological development and climate change impacts (Leclère et al. 2014). Output from the EPIC crop model is used to compute at each time step yields shifters for each climate change scenario and each crop and management system at a disaggregated spatial scale (pixel-level). Based on inputs from climate models (daily climatic conditions including solar radiation, min and max temperature, precipitation, wind speed, relative humidity and CO_2 concentration), EPIC simulates scenario-specific yields which are used together with historical values to compute the yield shifters. EPIC crop yield impacts, and their implementation in GLOBIOM, are further explained in Leclère et al. (2014) and Baker et al. (2018).

International trade International trade is represented through Enke-Samuelson-Takayama-Judge spatial equilibrium assuming homogenous goods (Takayama and Judge 1971). Bilateral trade flows are determined by the initial trade pattern, relative production costs of regions and the minimization of trading costs. Trade costs are composed of tariffs from the MAcMap-HS6 database (Bouët et al. 2008) and transport costs (Hummels 2001). A non-linear element is added in which trade costs increase with traded quantity to model persistency in trade flows via a constant elasticity function for trade flows observed in the base year, and a quadratic function for new trade flows. The non-linear element reflects the cost of trade expansion in terms of infrastructure and capacity constraints in the transport sector and is reset after each 10 year time step. Compared to other global economic models, GLOBIOM's trade representation is positioned between the rigid Armington approach of general equilibrium models and the flexible world pool market approach of many partial equilibrium models. Further information on the

international trade representation in GLOBIOM can be found in supplementary material of Baker et al. (2018).

Risk of hunger We use an indicator for the population at risk of hunger developed by Hasegawa et al. (2015). It is based on the FAO methodology in which the number of people at risk of hunger is calculated by multiplying the share of population at risk of hunger with the total population. The share of the population at risk of hunger is the proportion of the population whose food availability falls below the mean minimum dietary energy requirement. Three parameters are used to calculate this share: the mean minimum dietary energy requirements (MDER), the coefficient of variation (CV) of the distribution of food within a country and the mean food availability (kcal per capita per day). Minimum dietary energy requirements are exogenously calculated based on demographic composition (age, sex) of future population projections. Future changes in the inequality of food distribution among households within a region are also exogenous and follow a region's projected income growth. This is based on an estimated relationship between income and the CV of food distribution with observed historical national-level data. Food availability in kcal per capita per day is endogenously determined with GLOBIOM at the regional level. More information on the method can be found in Hasegawa et al. (2015; 2018).

Scenario design We simulate climate change scenarios corresponding to four representative concentration pathways (RCPs, 2.6 Wm^{-2} scenario, 4.5 Wm^{-2} scenario, 6 Wm^{-2} scenario and 8.5 Wm^{-2} scenario) (van Vuuren et al. 2011) as projected by the HadGEM2-ES general circulation model (GCM) (Martin et al. 2011; Collins et al. 2011). CO_2 fertilization effects are included in all RCPs and RCP8.5 is also implemented without CO_2 fertilization. RCP8.5 is furthermore implement with 4 additional GCMs to reflect uncertainty in climate models: GFDL-ESM2M (Dunne et al. 2012), IPSL-CM5A-LR (Dufresne et al. 2013), MIROC-ESM-CHEM (Watanabe et al. 2011), and NorESM1-M (Bentsen et al. 2013). The impact of corresponding climate changes on agricultural yields is based simulations from the crop model EPIC (Leclère et al. (2014), Baker et al. 2018). In the baseline scenario with no climate change (No_CC) exogenous change to crop yields originates only from long-term technological development assumptions.

We implement four trade scenarios to analyze the role of trade in climate change adaptation. The first scenario, *Fixed imports*, limits imports to be less than or equal to imports observed in the baseline scenario without climate change. This indicates what happens if adjustments in trade flows in response to climate change are restricted, thus limiting trade as an adaptation mechanism. In addition, we implement three trade integration scenarios to assess what happens if the trade adaptation mechanism is promoted. In the first scenario, *Facilitation* the non-linear part of trade costs is set close to zero, following the approach described in Baker et al. (2018). This reflects the impact of reducing transaction costs, infrastructure costs and other non-tariff barriers limiting the expansion of trade flows. In the second scenario, *Tariff elimination*, all agricultural tariffs are progressively phased out between 2020 and 2050, i.e. -25% in 2020, -50% in 2030, -75% in 2040 and -100% in 2050. The last one, *Facilitation + Tariff elimination,* is a combination of the previous two ones and presents the most extensive open trade scenario. In the *Baseline trade* scenario trade barriers are kept constant at their level in 2000, but trade patterns are allowed to vary endogenously across the different climate impact scenarios.

Socioeconomic developments are modelled according to the second Shared Socio-Economic Pathway (SSP2), which reflects a 'Middle of the Road' scenario where population reaches 9.2 billion by 2050 and income grows according to historical trends in each region (Fricko et al. 2017). The SSP scenarios have been discussed widely in the literature and are often used as a basis for harmonizing key macroeconomic

assumptions for integrated assessment modeling of different climate futures, e.g. Riahi et al. (2017). SSP2 projects a decrease in the global population at risk of hunger over time, from 867 million in 2000 to 163 million by 2050. This is because of an increase in food consumption and an improved food distribution within regions, which are in turn both related to the assumed income growth under SSP2 (Hasegawa, Fujimori, Takahashi, et al. 2015).

Statistical analysis We analyze the results from the scenario runs with a regional level linear regression model to infer the underlying relationship between trade costs, crop yield changes and hunger as predicted by GLOBIOM. The following two models are estimated by Ordinary Least Squares (OLS) (regression results in Table 1):

$$Population\ at\ risk\ of\ hunger_{itr} = \beta_1 Crop\ yield_{ir} + \beta_2\, Trade\ costs_{itr} + \beta_3 Crop\ yield_{ir} *\ Trade\ costs_{itr} + \beta_4 Region + \varepsilon$$

$$Food\ availability_{itr} = \beta_1 Crop\ yield_{ir} + \beta_2\, Trade\ costs_{itr} + \beta_3 Crop\ yield_{ir} *\ Trade\ costs_{itr} + \beta_4 Region + \varepsilon$$

Population at risk of hunger$_{itr}$ gives the number of people at risk of hunger (million) and *Food availability*$_{itr}$ the food availability (kcal/cap/day) in 2050 in each region i, trade scenario t and climate change scenario r. *Crop yield*$_{ir}$ gives the change in average crop yield (kcal/ha) compared to average crop yield in no climate change in 2050 for each region i and climate change scenario r. *Trade cost*$_{itr}$ gives the log of the weighted average trade costs (USD/kcal) on all trade flows in 2050 per region i, trade scenario t and climate change scenario r. *Region* is a categorical variable with 11 levels (USA, CAN, EUR, MNA, SEA, EAS, SSA, SAS, CSI, OCE, LAC). Further details on the regression, including the model with regional interaction effects (Figure 3 and SI Table 3), are included in the Supplementary Information (SI).

Comparative advantage When trade barriers are removed, Ricardo's trade theory predicts that countries produce and export relatively more of the goods for which they have a comparative advantage (Costinot, Donaldson, and Komunjer 2012). To assess comparative advantage we estimate a linear regression model of the effect of trade cost reduction on the share of a region's production in total world production for each crop, the share of each crop in a region's total crop production, and the share of a region's production that is exported. The following three models are estimated by Ordinary Least Squares (OLS) for each crop separately (regression results Figure 4 and Supplementary Figure 6 and 7):

$$Share\ of\ world\ production_{itr} = \beta_1\, Trade\ costs_{itr} *\ Region + \varepsilon$$

$$Share\ of\ regional\ crop\ production_{itr} = \beta_1\, Trade\ costs_{itr} *\ Region + \varepsilon$$

$$Share\ of\ production\ exported_{itr} = \beta_1\, Trade\ costs_{itr} *\ Region + \varepsilon$$

Share of world production$_{itr}$ gives the share of production of a crop that region i represents in total world production of the crop in each trade scenario t and climate change scenario r. *Share of regional crop production*$_{itr}$ share of production that a crop represents in total crop production of region i in each scenario (t,r). *Share of production exported*$_{itr}$ share of production of a crop that is exported in region i in each scenario (r,t). *Trade costs*$_{itr}$ is the log of weighted average of trade costs on exports (USD/ton) per region i, trade scenario t and climate change scenario r. *Region* is a categorical variable with 11 levels (USA, CAN, EUR, MNA, SEA, EAS, SSA, SAS, CSI, OCE, LAC). Further details on the regression are included in the SI.

These indicators take into account differences in land productivity, land endowment and price competitiveness between crops and regions. In the SI we report additional indicators including the relative

competitiveness across regions for each crop (Supplementary Figure 3) and the ratio of the yield of each crop compared to other crops between regions (Supplementary Figure 4) which reflects the pure Ricardo-based comparative advantage.

References

Baker, Justin, Petr Havlik, Robert Beach, David Leclère, Erwin Schmid, Hugo Valin, Jefferson Cole, Jared Creason, Sara Ohrel, and James McFarland. 2018. "Evaluating the Effects of Climate Change on US Agricultural Systems: Sensitivity to Regional Impact and Trade Expansion Scenarios." *Environmental Research Letters*, 0–48.

Baldos, Uris Lantz C, and Thomas W Hertel. 2015. "The Role of International Trade in Managing Food Security Risks from Climate Change." *Food Security*, 275–90. https://doi.org/10.1007/s12571-015-0435-z.

Bentsen, M., I. Bethke, J. B. Debernard, T. Iversen, A. Kirkev˚ag, Ø. Seland, C. Hoose, et al. 2013. "The Norwegian Earth System Model, NorESM1-M – Part 1: Description and Basic Evaluation of the Physical Climate." *Geoscientific Model Development* 6 (3): 687–720. https://doi.org/10.5194/gmd-6-687-2013.

Bouët, Antoine, Yvan Decreux, Lionel Fontagné, Sébastien Jean, and David Laborde. 2008. "Assessing Applied Protection across the World." *Review of International Economics* 16 (5): 850–63. https://doi.org/10.1111/j.1467-9396.2008.00753.x.

Brown, Molly E., Edward R. Carr, Kathryn L. Grace, Keith Wiebe, Christopher C. Funk, Witsanu Attavanich, Peter Backlund, and Lawrence Buja. 2017. "Do Markets and Trade Help or Hurt the Global Food System Adapt to Climate Change?" *Food Policy* 68: 154–59. https://doi.org/10.1016/j.foodpol.2017.02.004.

Collins, W. J., N. Bellouin, M. Doutriaux-Boucher, N. Gedney, P. Halloran, T. Hinton, J. Hughes, et al. 2011. "Development and Evaluation of an Earth-System Model – HadGEM2." *Geoscientific Model Development* 4 (4): 1051–75. https://doi.org/10.5194/gmd-4-1051-2011.

Costinot, Arnaud, Dave Donaldson, and Ivana Komunjer. 2012. "What Goods Do Countries Trade? A Quantitative Exploration of Ricardo's Ideas." *Review of Economic Studies* 79 (2): 581–608. https://doi.org/10.1093/restud/rdr033.

Costinot, Arnaud, Dave Donaldson, and Cory Smith. 2016. "Evolving Comparative Advantage and the Impact of Climate Change in Agricultural Markets: Evidence from 1.7 Million Fields around the World." *Journal of Political Economy* 124 (1): 205–48. https://doi.org/10.1086/684719.

Cui, Hao David, Marijke Kuiper, Hans van Meijl, and Andrzej Tabeau. 2018. "Climate Change and Global Market Integration: Implications for Global Economic Activities, Agricultural Commodities, and Food Security. The State of Agricultural Commodity Markets (SOCO) 2018: Background Paper." Rome: FAO.

Dufresne, J. L., M. A. Foujols, S. Denvil, A. Caubel, O. Marti, O. Aumont, Y. Balkanski, et al. 2013. *Climate Change Projections Using the IPSL-CM5 Earth System Model: From CMIP3 to CMIP5*. *Climate Dynamics*. Vol. 40. https://doi.org/10.1007/s00382-012-1636-1.

Dunne, John P., Jasmin G. John, Alistair J. Adcroft, Stephen M. Griffies, Robert W. Hallberg, Selena Shevliakova, Ronald J. Stouffer, et al. 2012. "GFDL's ESM2 Global Coupled Climate-Carbon Earth

System Models. Part I: Physical Formulation and Baseline Simulation Characteristics." *Journal of Climate* 25: 6646–65. https://doi.org/http://dx.doi.org/10.1175/JCLI-D-11-00560.1.

FAO, IFAD, UNICEF, WFP, and WHO. 2018. *The State of Food Security and Nutrition in the World 2018. Building Climate Resilience for Food Security and Nutrition*.

Fricko, Oliver, Petr Havlik, Joeri Rogelj, Zbigniew Klimont, Mykola Gusti, Nils Johnson, Peter Kolp, et al. 2017. "The Marker Quantification of the Shared Socioeconomic Pathway 2: A Middle-of-the-Road Scenario for the 21st Century." *Global Environmental Change* 42: 251–67. https://doi.org/10.1016/j.gloenvcha.2016.06.004.

Gouel, Christophe, and David Laborde. 2018. "The Crucial Role of International Trade in Adaptation to Climate Change."

Hasegawa, Tomoko, Shinichiro Fujimori, Petr Havlík, Hugo Valin, Benjamin Leon Bodirsky, Jonathan C. Doelman, Thomas Fellmann, et al. 2018. "Risk of Increased Food Insecurity under Stringent Global Climate Change Mitigation Policy." *Nature Climate Change* 8 (8): 699–703. https://doi.org/10.1038/s41558-018-0230-x.

Hasegawa, Tomoko, Shinichiro Fujimori, Yonghee Shin, Akemi Tanaka, Kiyoshi Takahashi, and Toshihiko Masui. 2015. "Consequence of Climate Mitigation on the Risk of Hunger." *Environmental Science and Technology* 49 (12): 7245–53. https://doi.org/10.1021/es5051748.

Hasegawa, Tomoko, Shinichiro Fujimori, Kiyoshi Takahashi, and Toshihiko Masui. 2015. "Scenarios for the Risk of Hunger in the Twenty-First Century Using Shared Socioeconomic Pathways." *Environmental Research Letters* 10 (1). https://doi.org/10.1088/1748-9326/10/1/014010.

Havlík, Petr, Hugo Valin, Mykola Gusti, Erwin Schmid, David Leclère, Nicklas Forsell, Mario Herrero, et al. 2015. "Climate Change Impacts and Mitigation in the Developing World, An Integrated Assessment of the Agriculture and Forestry Sectors. Background Paper for the World Bank Report: 'Shock Waves: Managing the Impacts of Climate Change on Poverty.'" 7477. Policy Research Working Paper.

Hertel, Thomas W. 2018. *Climate Change, Agricultural Trade and Global Food Security. The State of Agricultural Commodity Markets (SOCO) 2018: Background Paper*. Vol. 9. Rome: FAO.

Hoegh-Guldberg, O., D. Jacob, M. Taylor, M. Bindi, S. Brown, I. Camilloni, A. Diedhiou, et al. 2018. "Impacts of 1.5°C of Global Warming on Natural and Human Systems." In *Global Warming of 1.5°C. An IPCC Special Report on the Impacts of Global Warming of 1.5°C above Pre-Industrial Levels and Related Global Greenhouse Gas Emission Pathways, in the Context of Strengthening the Global Response to the Threat of Climate Change,*.

Huang, Hsin, Martin von Lampe, and Frank van Tongeren. 2011. "Climate Change and Trade in Agriculture." *Food Policy* 36 (SUPPL. 1): S9–13. https://doi.org/10.1016/j.foodpol.2010.10.008.

Hummels, David. 2001. "Toward a Geography of Trade Costs."

Leclère, D., P. Havlík, S. Fuss, E. Schmid, A. Mosnier, B. Walsh, H. Valin, M. Herrero, N. Khabarov, and M. Obersteiner. 2014. "Climate Change Induced Transformations of Agricultural Systems: Insights from a Global Model." *Environmental Research Letters* 9 (12). https://doi.org/10.1088/1748-9326/9/12/124018.

Martin, G. M., N. Bellouin, W. J. Collins, I. D. Culverwell, P. R. Halloran, S. C. Hardiman, T. J. Hinton, et al.

2011. “The HadGEM2 Family of Met Office Unified Model Climate Configurations.” *Geoscientific Model Development* 4 (3): 723–57. https://doi.org/10.5194/gmd-4-723-2011.

Mosnier, Aline, Michael Obersteiner, Petr Havlík, Erwin Schmid, Nikolay Khabarov, Michael Westphal, Hugo Valin, Stefan Frank, and Franziska Albrecht. 2014. “Global Food Markets, Trade and the Cost of Climate Change Adaptation.” *Food Security*, 29–44. https://doi.org/10.1007/s12571-013-0319-z.

Nelson, Gerald C., Hugo Valin, Ronald D. Sands, Petr Havlík, Helal Ahammad, Delphine Deryng, Joshua Elliott, et al. 2014. “Supporting Information - Climate Change Effects on Agriculture: Economic Responses to Biophysical Shocks.” *PNAS* 111 (9): 2396–2407. https://doi.org/10.1107/S1600536809047072.

Riahi, Keywan, Detlef P. van Vuuren, Elmar Kriegler, Jae Edmonds, Brian C. O’Neill, Shinichiro Fujimori, Nico Bauer, et al. 2017. “The Shared Socioeconomic Pathways and Their Energy, Land Use, and Greenhouse Gas Emissions Implications: An Overview.” *Global Environmental Change* 42: 153–68. https://doi.org/10.1016/j.gloenvcha.2016.05.009.

Rosenzweig, Cynthia, Joshua Elliott, Delphine Deryng, Alex C. Ruane, Christoph Müller, Almut Arneth, Kenneth J. Boote, et al. 2014. “Assessing Agricultural Risks of Climate Change in the 21st Century in a Global Gridded Crop Model Intercomparison.” *Proceedings of the National Academy of Sciences* 111 (9): 3268–73. https://doi.org/10.1073/pnas.1222463110.

Stevanović, Miodrag, Alexander Popp, Hermann Lotze-Campen, Jan Philipp Dietrich, Christoph Müller, Markus Bonsch, Christoph Schmitz, Benjamin Bodirsky, Florian Humpenöder, and Isabelle Weindl. 2016. “The Impact of High-End Climate Change on Agricultural Welfare.” *Science Advances*, no. August: 1–10.

Vuuren, Detlef P. van, Jae Edmonds, Mikiko Kainuma, Keywan Riahi, Nebojsa Nakicenovic, Steven J Smith, and Steven K Rose. 2011. “The Representative Concentration Pathways: An Overview.” *Climatic Change* 109: 5–31. https://doi.org/10.1007/s10584-011-0148-z.

Watanabe, S., T. Hajima, K. Sudo, T. Nagashima, T. Takemura, H. Okajima, T. Nozaw, et al. 2011. “MIROC-ESM 2010: Model Description and Basic Results of CMIP5-20c3m Experiments.” *Geoscientific Model Development* 4 (4): 845–72. https://doi.org/10.5194/gmd-4-845-2011.

Wiebe, Keith, Hermann Lotze-Campen, Ronald Sands, Andrzej Tabeau, Dominique Van Der Mensbrugghe, Anne Biewald, Benjamin Bodirsky, et al. 2015. “Climate Change Impacts on Agriculture in 2050 under a Range of Plausible Socioeconomic and Emissions Scenarios.” *Environmental Research Letters* 10 (8). https://doi.org/10.1088/1748-9326/10/8/085010.

Supplementary Information

Global hunger and climate change adaptation through international trade

Janssens Charlotte[1,2], Havlik Petr[1], Krisztin Tamas[1], Baker Justin[3], Tomoko Hasegawa[1,4], Nicole Van Lipzig[2], Miet Maertens[2]

[1] International Institute for Applied System Analysis (IIASA), Schlossplatz 1, A-2361 Laxenburg, Austria
[2] University of Leuven (KU Leuven), Department of Earth and Environmental Sciences, Celestijnenlaan 200E, Heverlee, Belgium
[3] RTI International, 3040 East Cornwallis Road, Durham, NC 27709-2194, United States of America
[4] Center for Social and Environmental Systems Research, National Institute for Environmental Studies (NIES), National Institute for Environmental Studies, 16–2 Onogawa, Tsukuba, Ibaraki 305–8506, Japan

Contents

Supplementary Method

1. Trade costs in GLOBIOM

Bilateral trade flows are determined by the initial trade pattern, relative production costs of regions and the minimization of trading costs. Trade costs are composed of tariffs from the MAcMap-HS6 database (Bouët, Decreux, Fontagné, Jean, & Laborde, 2008), transport costs (Hummels, 2001) and a non-linear element in which trade costs increase with traded quantity to model persistency in trade flows. The latter element reflects the cost of trade expansion in terms of infrastructure and capacity constraints in the transport sector and is reset after each 10 year time step. The implication of the trade scenarios for production, trade patterns and trade costs varies across crops and regions because the level of initial trade barriers is for example different. The impact differs also across climate change scenarios through the dependency of trade on the competitiveness of each region. The spatial price equilibrium approach implies that trade will occur when the cost of trade between two regions is smaller than the regional price difference, and this price difference will become equal to the marginal trade cost in equilibrium (McCarl & Spreen, 2002). We aggregate these computed trade costs on each trade flow to obtain a measure that reflects the implication of trade scenarios on overall trading costs for each crop and region. GLOBIOM models bilateral trade flows and trade costs at the level of 30 sub-regions. To be in line with the level of analysis of the paper, we aggregate this information to the level of 11 regions (USA, CAN, EUR, MNA, SEA, EAS, SSA, SAS, CSI, OCE, LAC). The correspondence between country, sub-region and region level is shown in Supplementary Table 4.

For the analysis on hunger (see also section 2.1) we calculate the weighted average over all agricultural imports, exports and intra-regional trade flows for each region i, trade scenario t and climate change scenario r:

$$average\ trade\ cost_{itr} = \sum_{k} \frac{x_{iktr}}{total\_x_{itr}} * trade\ cost_{iktr}$$

where x_{iktr} are the trade flows of crop k in, out and within region i in each scenario (t,r) and $total\_x_{itr}$ is the sum of all trade flows in, out and within region i in each scenario (t,r).

For the analysis on comparative advantage (see also section 2.2), we calculate a weighted average of trade cost on exports of crop k, region i, trade scenario t and climate change scenario r:

$$average\ trade\ cost_{iktr} = \sum_{l \in i, j \notin i} \frac{x_{ljktr}}{x_{iktr}} * trade\ cost_{ljktr}$$

where x_{ljktr} are export flows of crop k from sub-region l ($\in region\ i$) to sub-region j ($\notin region\ i$) in each scenario (t,r) and x_{iktr} is the total export of crop k from sub-regions l to sub-regions j in each scenario (t,r).

2. Statistical analysis

Hunger and food availability regression analysis

The following regression models with regional fixed effects are estimated with OLS (results in Table 1):

$$Population\ at\ risk\ of\ hunger_{itr} = \beta_1 Crop\ yield_{ir} + \beta_2\, Trade\ costs_{itr} + \beta_3 Crop\ yield_{ir} *\ Trade\ costs_{itr} + \beta_4 Region + \varepsilon$$

$$Food\ availability_{itr} = \beta_1 Crop\ yield_{ir} + \beta_2\, Trade\ costs_{itr} + \beta_3 Crop\ yield_{ir} *\ Trade\ costs_{itr} + \beta_4 Region + \varepsilon$$

with

- *Population at risk of hunger*$_{itr}$: continuous variable that gives the number of people at risk of hunger (million) in 2050 in region i, trade scenario t and climate change scenario r.
- *Food availability*$_{itr}$: continuous variable that gives the food availability (kcal/cap/day) in 2050 in region i, trade scenario t and climate change scenario r.
- *Region*: categorical variable with 11 levels (USA, CAN, EUR, MNA, SEA, EAS, SSA, SAS, CSI, OCE, LAC)
- *Crop yield*$_{ir}$: continuous variable that gives percentage change in average crop yield (kcal/ha) compared to crop yield in no climate change in 2050 for each region i and climate change scenario r. This variable is centered (demeaned) to solve structural multicollinearity.
- *Trade costs*$_{jtr}$: continuous variable that gives the logarithm of the weighted average trade costs (USD/kcal) on all trade flows in 2050 per region i, trade scenario t and climate change scenario r. Trade costs are weighted based on the trade quantity of each trade flow in and out of a region. This variable is centered (demeaned) to solve structural multicollinearity.

Standard errors are estimated robust to heteroscedasticity using the HC3 method as recommended by Long and Ervin (2000)[1]. The F statistic of overall significance rejects null hypothesis at 1% significance level for both models. Summary statistics of the dependent and explanatory variables are shown in Table 1 below.

Supplementary Method Table 1 | Descriptive statistics of the dependent and explanatory variables (at regional level). The sample is composed of observations for the 11 regions for the 5 trade scenarios, the no climate change scenario and the 9 climate change scenarios. Two outliers in terms of trade costs are removed: [EUR, T1, 8p5wo] and [CSI, T1, 8p5wo]. This leads to 548 observations (= 11 regions x 5 trade scenarios x 10 RCP-GCM scenarios – 2 outliers).

	Min	Average	Max
Population at risk of hunger (million)	0	14.19	87.63
Food availability (kcal/cap/day)	1758	2230	2655
Crop yield (difference with NoCC)	-38%	-5%	+36%
Trade costs (US$/$10^6$ kcal)	15.09	67.60	221.67

[1] HC3 is a refined version of White's method for estimation of heteroskedastic standard errors (HC0). Long and Ervin (2000) demonstrate with Monte Carlo simulations that the HC3 method outperforms HC0 for small sample sizes (N < 250).

The following regression models with regional interaction terms are estimated with OLS (results in Figure 3 and Supplementary Table 3):

$$Population\ at\ risk\ of\ hunger_{itr} = \beta_1 Crop\ yield_{ir} * Region + \beta_2\ Trade\ costs_{itr} * Region + \beta_3 Crop\ yield_{ir} *\ \ Trade\ costs_{itr} * Region + \ \varepsilon$$

$$Food\ availability_{itr} = \beta_1 Crop\ yield_{ir} * Region + \beta_2\ Trade\ costs_{itr} * Region + \beta_3 Crop\ yield_{ir} *\ \ Trade\ costs_{itr} * Region + \ \varepsilon$$

with variables as for the model with regional fixed effects.

Standard errors are estimated robust to heteroscedasticity using the HC3 method. The calculation of regional interaction effects is done with the Delta Method. In specific, we calculate the interaction effects between regional dummies and the continuous variables. The regional fixed effect is not added to the interaction effect because we are interested for example in the effect of exogenous crop yield change on hunger in each region, without including the effect of being a certain region on hunger. The sample is composed of observations for 9 regions for the 5 trade scenarios, the no climate change scenario and the 9 climate change scenarios. One outlier in terms of trade costs are removed: [CSI, T1, 8p5wo]. This leads to 449 observations (= 9 regions x 5 trade scenarios x 10 RCP-GCM scenarios – 1 outliers). The F statistic of overall significance rejects null hypothesis at 1% significance level for both models.

Comparative advantage regression analysis

The following models are estimated with OLS for corn, soya, rice and wheat (results in Figure 4 and Supplementary Figures 6 and 7):

$$Share\ of\ world\ production_{itr} = \beta_1\ Trade\ costs_{itr} *\ \ Region + \ \varepsilon$$

$$Share\ of\ regional\ crop\ production_{itr} = \beta_1\ Trade\ costs_{itr} *\ \ Region + \ \varepsilon$$

$$Share\ of\ production\ exported_{itr} = \beta_1\ Trade\ costs_{itr} *\ \ Region + \ \varepsilon$$

with

- *Share of world production*$_{iktr}$: share of production that region i represents in total world production of the crop in each scenario (t,r) in 2050 (ranges between [0, 1]).
- *Share of specific crop in total regional crop production*$_{iktr}$: share of production that the crop represents in total crop production of region i in each scenario (t,r) in 2050 (ranges between [0, 1]).
- *Share of production that is exported*$_{iktr}$: share of production of the crop that is exported in region i in each scenario (r,t) in 2050 (ranges between [0, 1]).
- *Region*: categorical variable with 11 levels (USA, CAN, EUR, MNA, SEA, EAS, SSA, SAS, CSI, OCE, LAC)
- *Trade costs*$_{iktr}$: log of the weighted average trade costs on exports (USD/ton) in 2050 for the crop per region i, trade scenario t and climate change scenario r. Trade costs are weighted based on the trade quantity of each export flow. This variable is centered (demeaned) to solve structural multicollinearity.

The regressions are estimated with three different samples: only no climate change scenario included (Figures Xa), only climate change scenarios included (Figures Xb) or only climate change scenarios with as the dependent variable the difference in outcome variable between climate change and no climate change (Figures Xc). Standard errors are estimated robust to heteroscedasticity using the HC3 method and the calculation of the regional interaction effect is done with the Delta Method.

Supplementary Figures

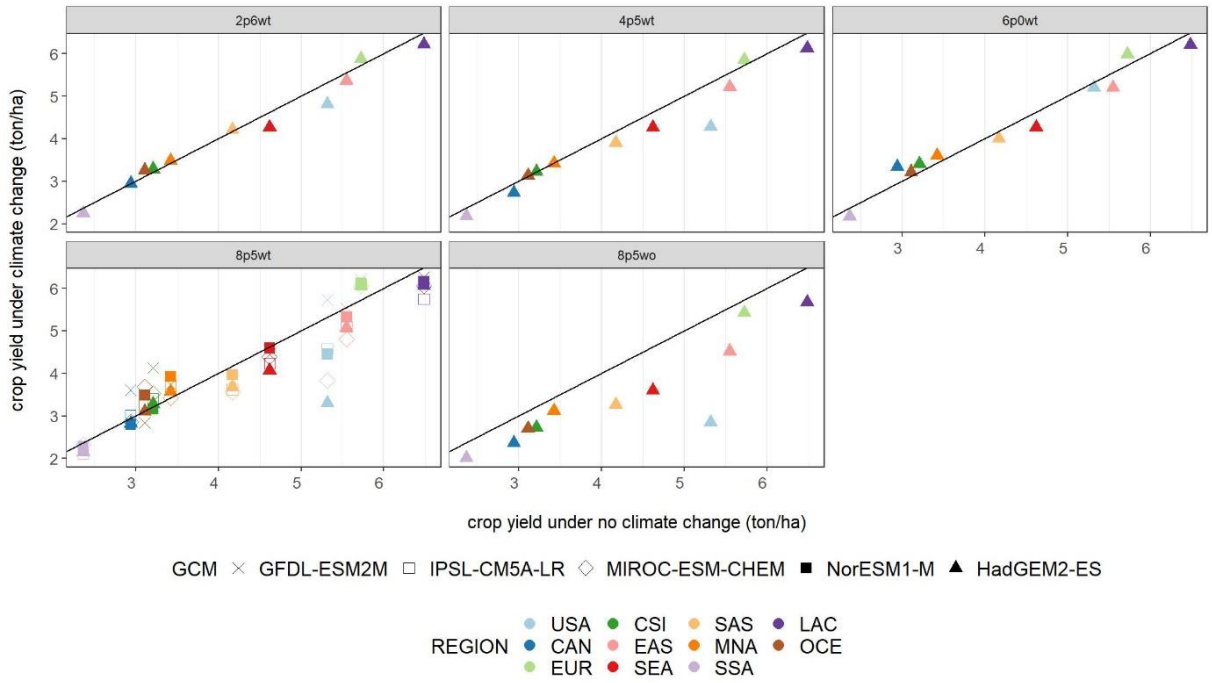

Supplementary Figure 1 | Impact of climate change on average crop yield in each region by 2050. The x-axis indicates the crop yield under no climate change (without GLOBIOM market feedback, determined by assumption on technological development) and y-axis the crop yield as projected by the EPIC crop model under climate change for different RCP x GCM combinations (without adaptation measures). Points above the black line indicate an increase in crop yield, points below a decrease in crop yield.

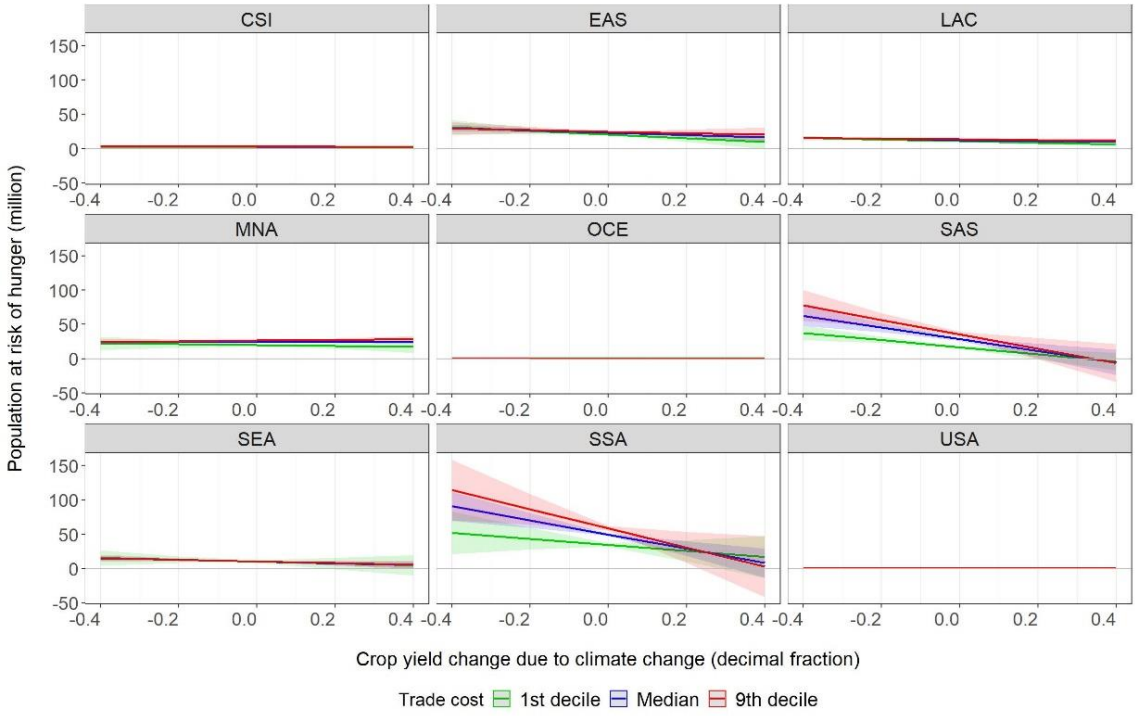

Supplementary Figure 2 | Plot of the fitted linear response of population at risk of hunger (million) to climate-induced crop yield change for different values of trade costs (1st decile, median, 9th decile). Shaded areas indicate prediction intervals. Prediction based on an OLS estimation of a regional level linear regression of the impact of crop yield change, trade costs and their interaction on population at risk of hunger. Regression results are shown in Supplementary Table 3 and the regression model is described in online and Supplementary Methods.

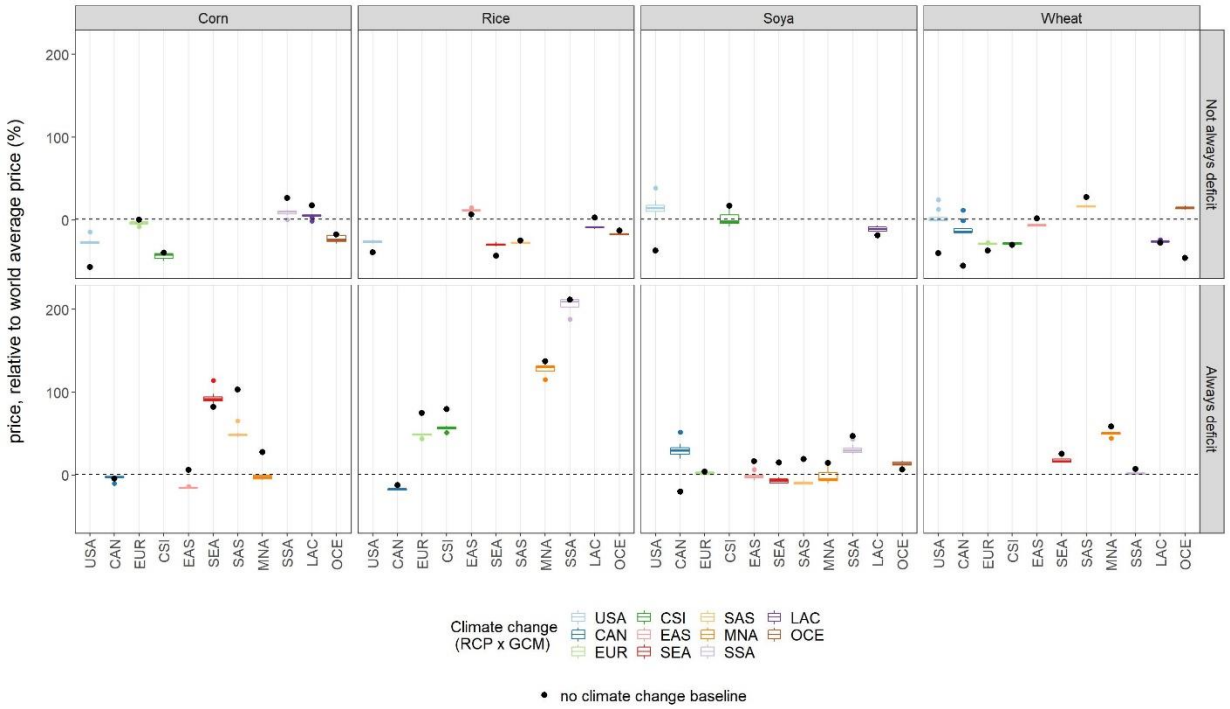

Supplementary Figure 3 | Relative competitiveness (across regions) in response to climate change in 2050 under the *Facilitation + Tariff elimination* scenario. The y axis indicates the producer price relative to the world average producer price for each crop, with values below zero indicating an above average competitiveness. The black dot indicates the relative producer price under no climate change, while the boxplot the relative producer price over the 9 climate change scenarios. Distinction is made between regions that have a deficit production in each trade and climate change scenario (*Always deficit*), and regions that do not (*Not always deficit*).

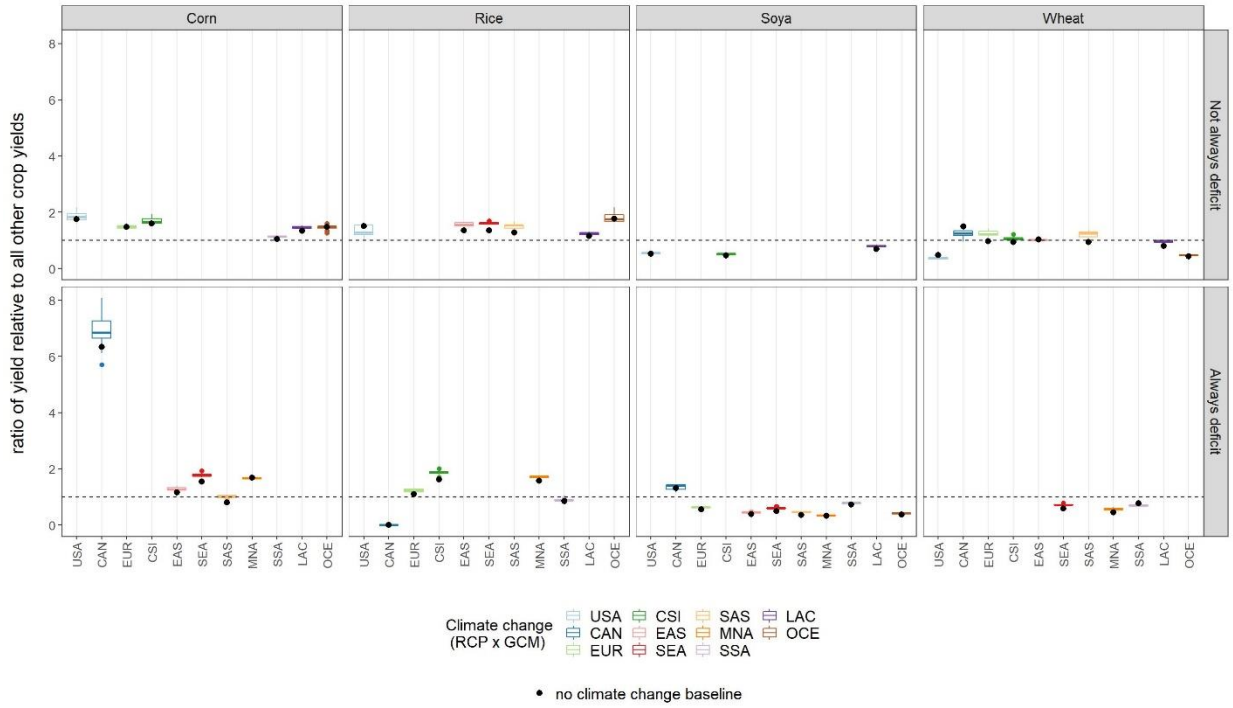

Supplementary Figure 4 | Relative yield of corn, rice, soya and wheat in response to climate change in 2050 under the *Baseline trade* scenario. The y-axis indicates for each crop the ratio of yield to the average yield of all other crops. A ratio larger than 1 (above the dotted line) indicates a low opportunity cost in terms of land. The black dot indicates the ratio in the no climate change scenario, while the boxplots the ratio under the 9 climate change scenarios. Distinction is made between regions that have a deficit production in each trade and climate change scenario (*Always deficit*), and regions who do not (*Not always deficit*).

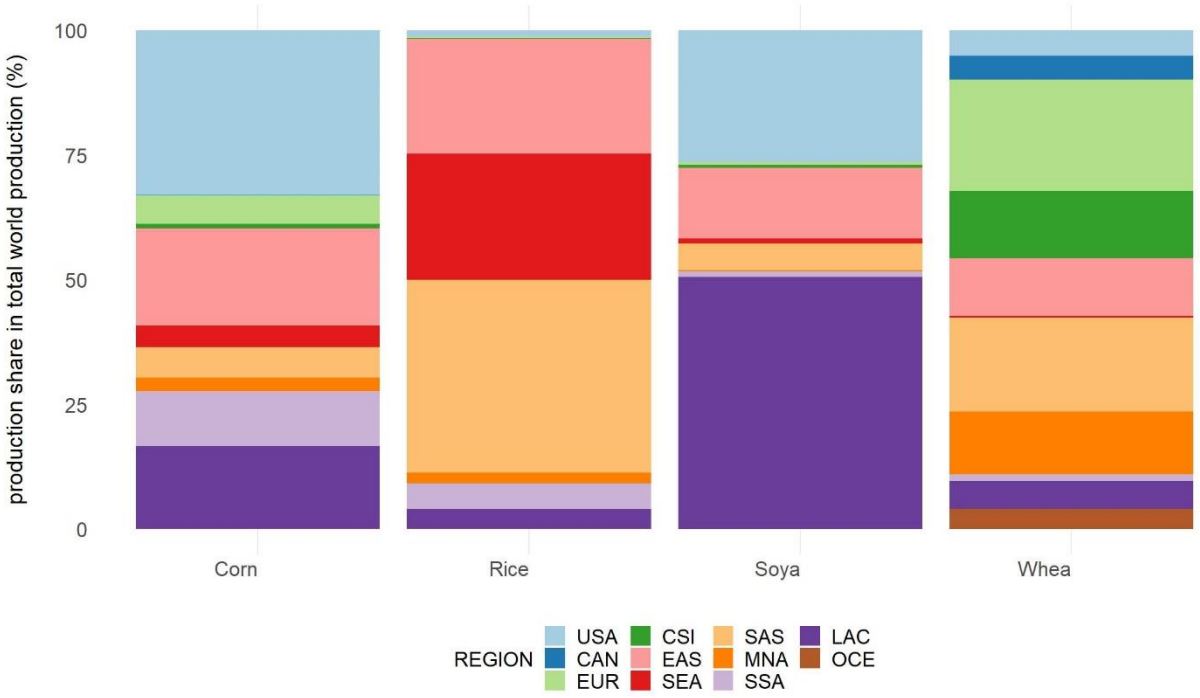

Supplementary Figure 5 | Share of production volume that each region represents of total world production for corn, rice, soya and wheat in the SSP2 baseline in 2050.

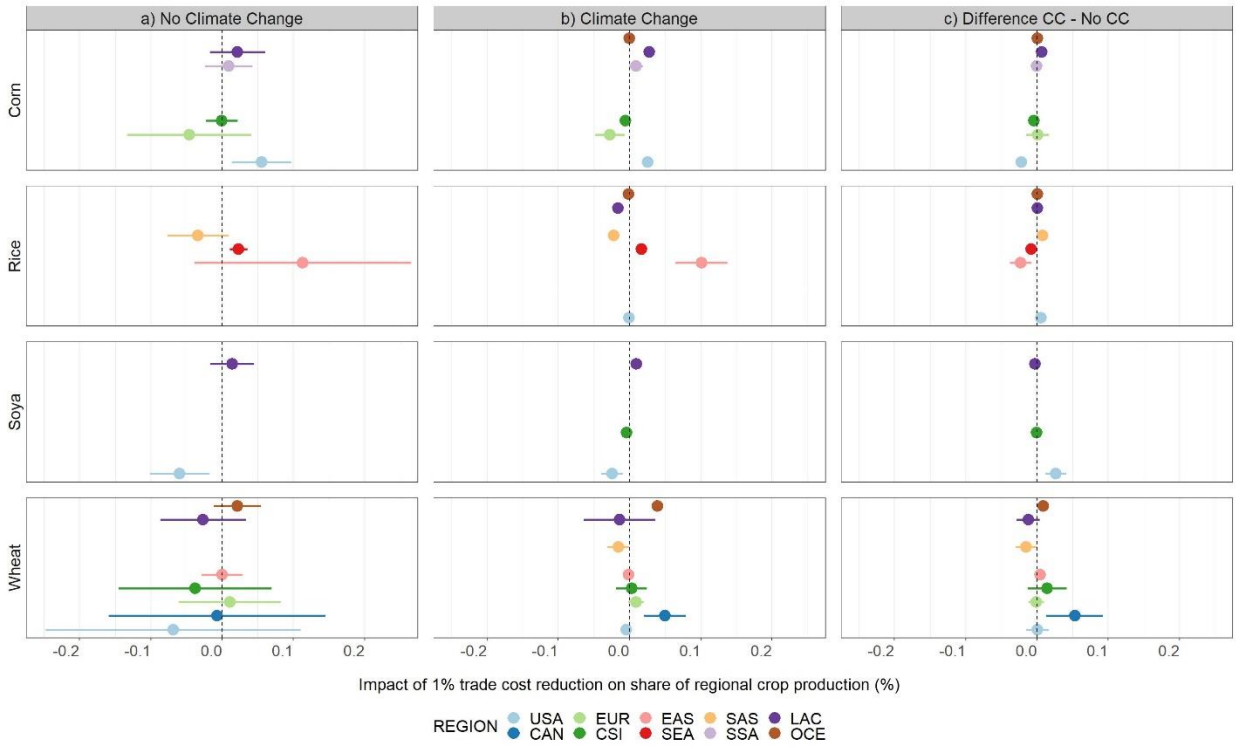

Supplementary Figure 6 | Intra-regional specialization in corn, rice, soya and wheat in response to trade cost reduction in 2050 under a) constant climate, b) climate change, and c) the difference between climate change and no climate change. Each subplot presents the results of an OLS estimation of a regional level linear regression model on the impact of export trade costs on share of a particular crop in total regional crop production. Each point shows the estimated impact of a 1% reduction in trade costs for a particular crop and region on share of regional crop production in percentage, with lines denoting the corresponding 95% confidence interval (heteroskedastic robust standard errors). For **a)** observations are taken from the constant climate change scenario and 4 trade scenarios (*Baseline trade, Facilitation, Tariff, Facilitation + Tariff*). Only regions are selected where the share of production of the crop in total regional crop production in the baseline is larger than 2%, and which have a surplus production of the crop in at least one of the three trade integration scenarios. N is 20 for corn, 12 for rice, 8 for soya, and 27 for wheat. For **b) and c)** observations are taken from the 9 climate change scenarios and 4 trade scenarios (*Baseline trade, Facilitation, Tariff, Facilitation + Tariff*) with exclusion of regions that have a deficit production in each trade and climate change scenario. N is 215 for corn, 216 for rice, 108 for soya and 263 for wheat. For **c)** the outcome variable is the difference in share of regional crop production with the no climate change scenario. The regression models are described in the online and Supplementary Methods.

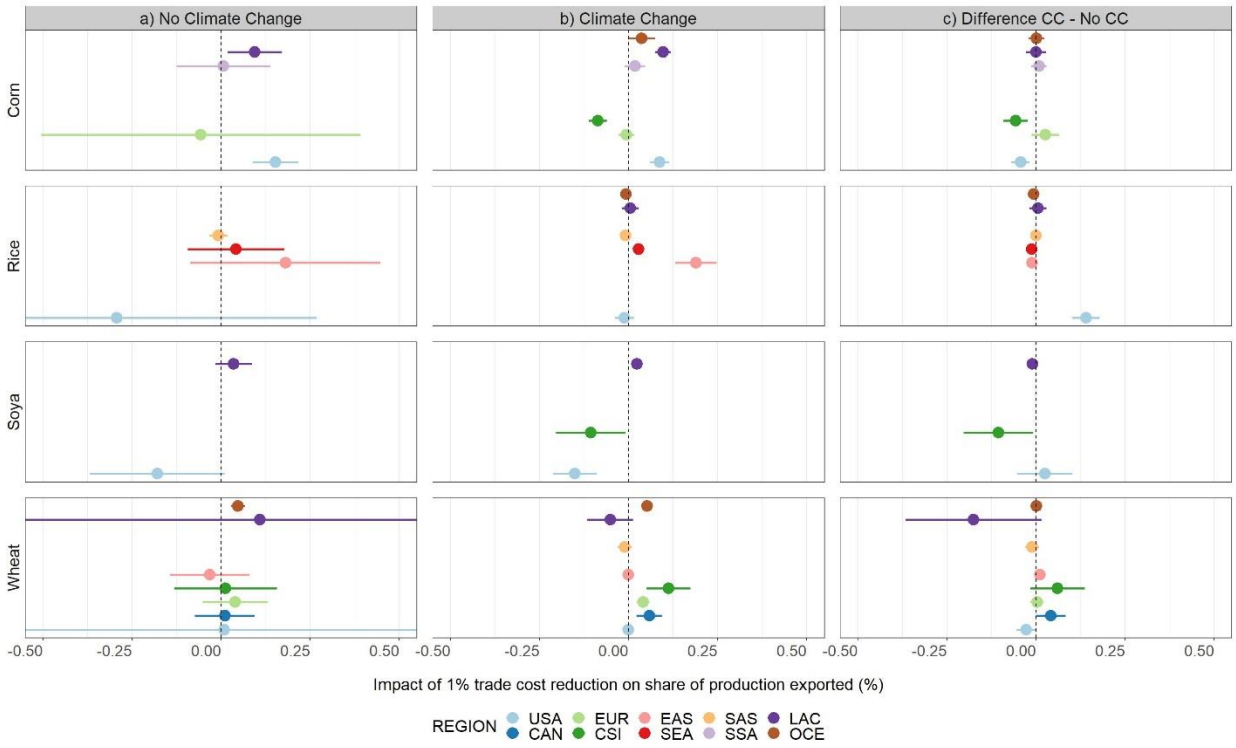

Supplementary Figure 7 | Export orientation of production in corn, rice, soya and wheat in response to trade cost reduction in 2050 under a) constant climate, b) climate change, and c) the difference between climate change and no climate change. Each subplot presents the results of a crop-specific OLS estimation of a regional level linear regression model on the impact of export trade costs on share of production exported. Each point shows the estimated impact of a 1% reduction in trade costs for a particular crop and region on share of production exported in percentage, with lines denoting the corresponding 95% confidence interval (heteroskedastic robust standard errors). For **a)** observations are taken from the constant climate change scenario and 4 trade scenarios (*Baseline trade, Facilitation, Tariff, Facilitation + Tariff*). Only regions are selected whose share of world production of the crop in the baseline is larger than 1%, and which have a surplus production of the crop in at least one of the three trade integration scenarios. 95% confidence interval of USA – rice is [-0.85, 0.27], of LAC – wheat [-0.69, 0.90] and of USA – wheat [-0.57, 0.59]. N is 16 for corn, 16 for rice, 8 for soya, and 27 for wheat. For **b) and c)** observations are taken from the 9 climate change scenarios and 4 trade scenarios (*Baseline trade, Facilitation, Tariff, Facilitation + Tariff*) with exclusion of regions that have a deficit production in each trade and climate change scenario. N is 215 for corn, 216 for rice, 108 for soya, and 263 for wheat. For **c)** the outcome variable is the difference in share of production exported with the no climate change scenario. The regression models are described in the online and Supplementary Methods.

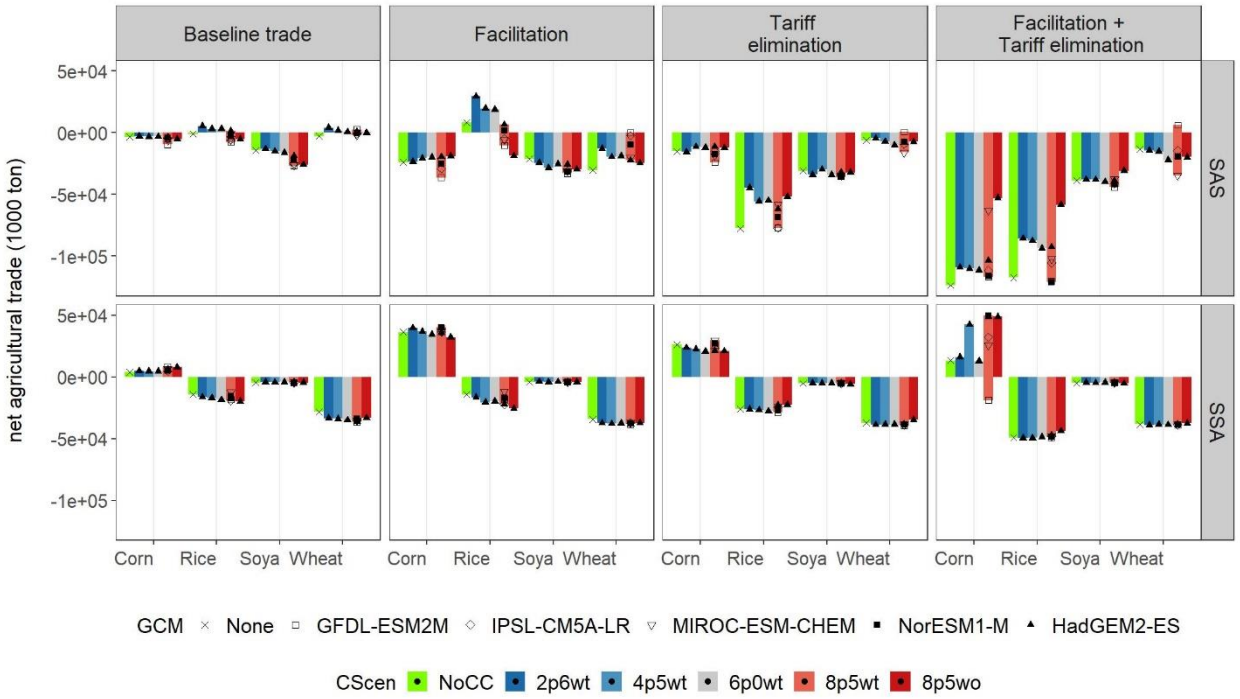

Supplementary Figure 8 | Net trade (1000 ton) in South Asia (SAS) and Sub-Saharan Africa (SSA) for corn, rice, soya and wheat under climate change and trade scenarios in 2050. Values above zero indicate net exports, while negative values indicate net imports.

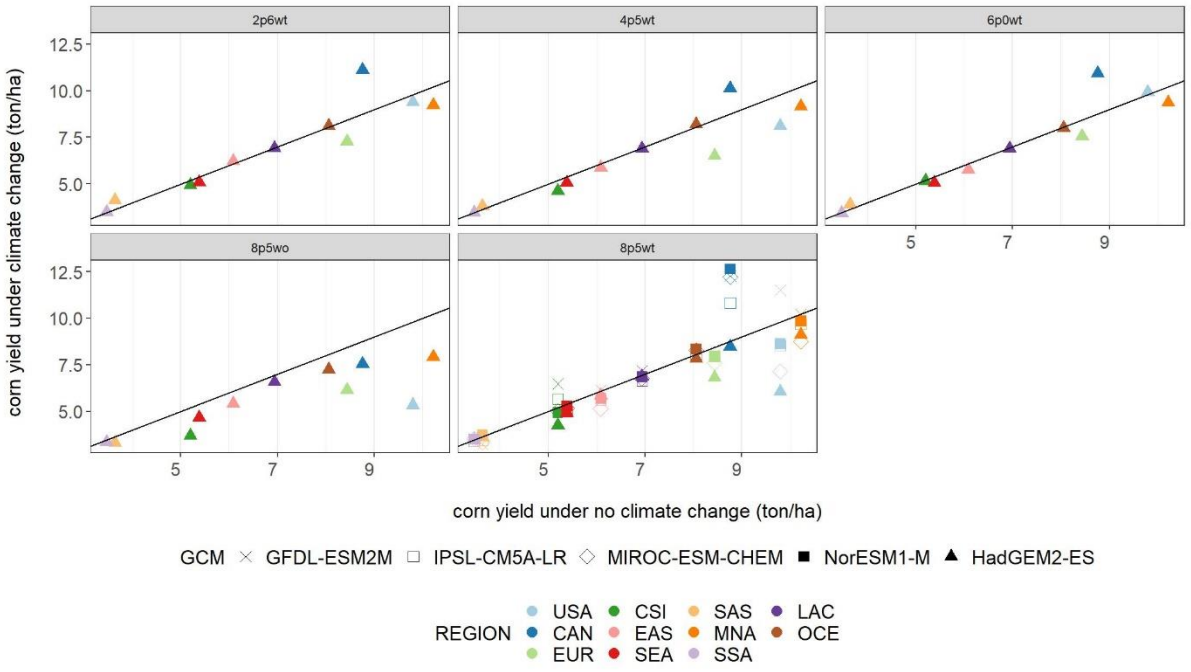

Supplementary Figure 9 | Corn yield (ton/ha) under climate change and under no climate change in each region based on projections by the EPIC crop model in 2050. Under no climate change crop yields are determined by base year yields and assumptions on technological development over time.

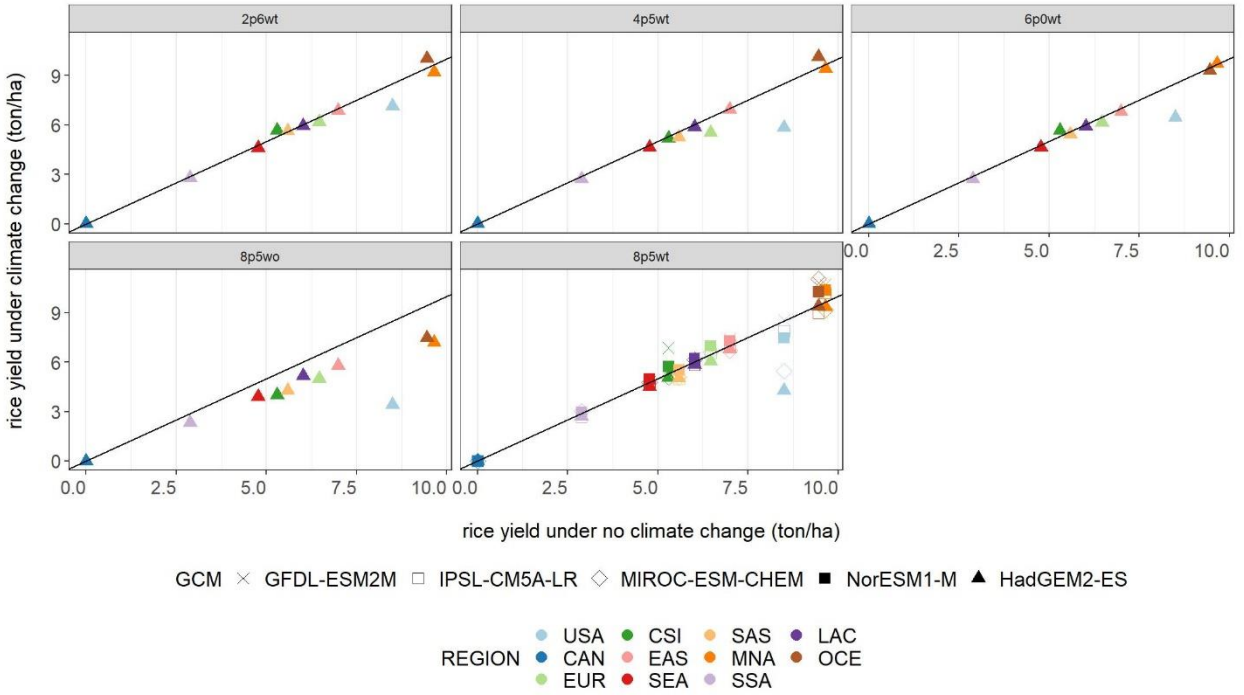

Supplementary Figure 10 | Rice yield under climate change and no climate change in each region as projected by the EPIC crop model in 2050. Under no climate change crop yields are determined by base year yields and assumptions on technological development over time.

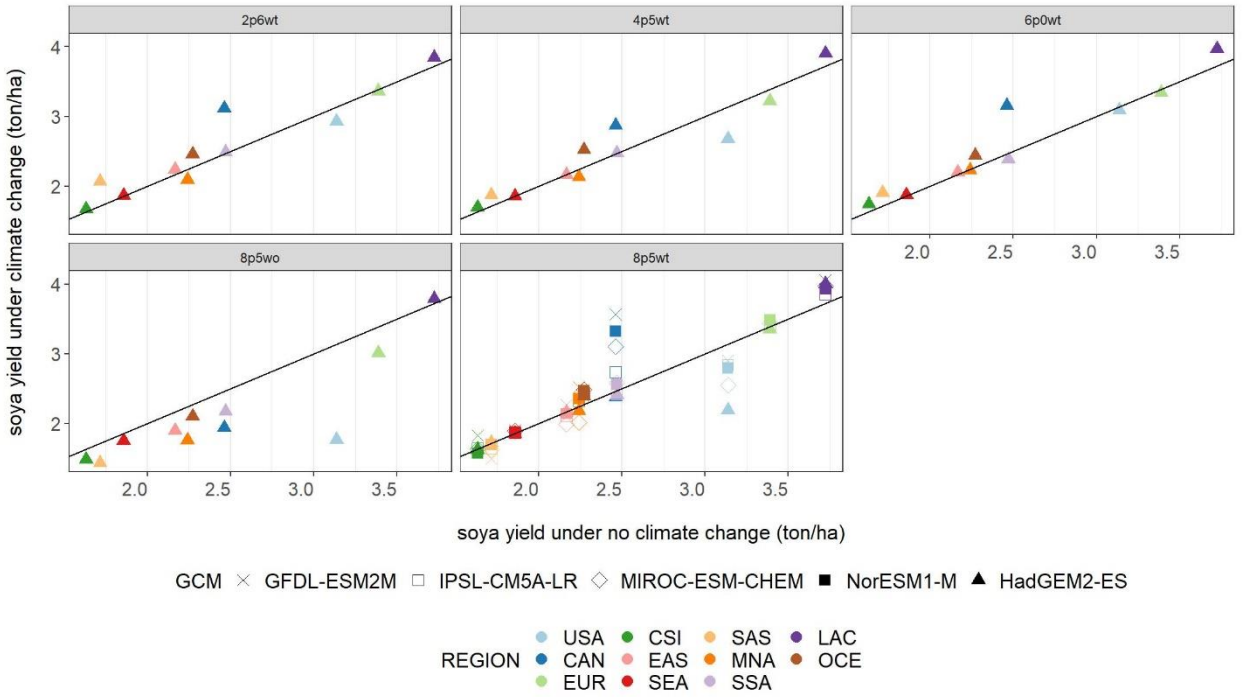

Supplementary Figure 11 | Soya yield under climate change and no climate change in each region as projected by the EPIC crop model in 2050. Under no climate change crop yields are determined by base year yields and assumptions on technological development over time.

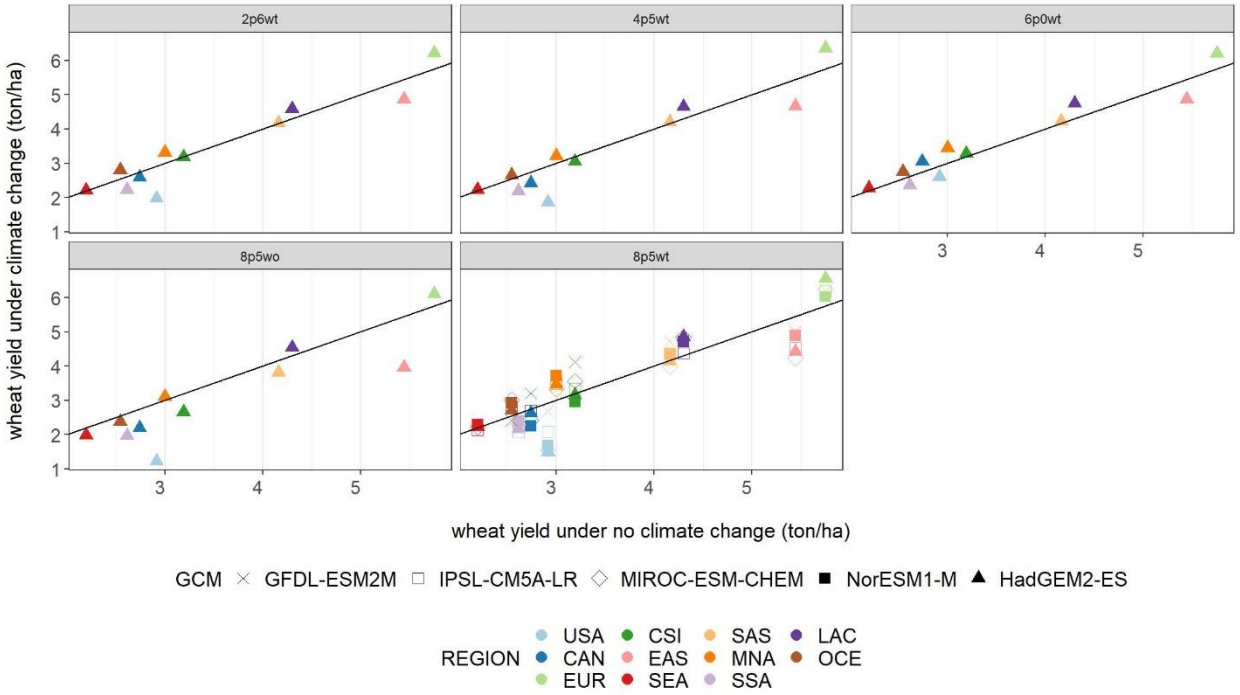

Supplementary Figure 12 | Wheat yield under climate change and no climate change in each region as projected by the EPIC crop model in 2050. Under no climate change crop yields are determined by base year yields and assumptions on technological development over time.

Supplementary Tables

Supplementary Table 2 | Global trade adjustments under trade and climate change scenarios compared to the SSP2 baseline computed by GLOBIOM by 2050. Total trade growth and specific extensive margin trade growth, the latter indicated as new trade flows compared to the 2000 trade pattern and new trade flows compared to the baseline SSP2 trade pattern. RCP: Representative Concentration Pathway, with (wt) or without (wo) CO_2 fertilization effect. GCM: General Circulation Model.

			Trade adjustments			
RCP	GCM	Trade scenario	Total trade volume (1000 ton)	Difference in total trade w.r.t. baseline (%)	Total volume of new trade flows w.r.t. 2000 (1000 ton)	Total volume of new trade flows w.r.t. baseline (1000 ton)
NoCC	None	Baseline	1317834	0	18727	0
2p6wt	HadGEM2-ES	Baseline	1359078	0.03	20991	13240
4p5wt	HadGEM2-ES	Baseline	1375502	0.04	22346	14634
6p0wt	HadGEM2-ES	Baseline	1383007	0.05	22529	19376
8p5wt	GFDL-ESM2M	Baseline	1471206	0.12	19937	7485
8p5wt	HadGEM2-ES	Baseline	1401549	0.06	25142	31346
8p5wt	IPSL-CM5A-LR	Baseline	1429006	0.08	22770	12219
8p5wt	MIROC	Baseline	1480669	0.12	19782	32376
8p5wt	NorESM1-M	Baseline	1348113	0.02	19942	17856
8p5wo	HadGEM2-ES	Baseline	1497331	0.14	29199	37426
NoCC	None	Fixed imports	1317191	0.00	18726	0
2p6wt	HadGEM2-ES	Fixed imports	1189833	-0.10	17319	0
4p5wt	HadGEM2-ES	Fixed imports	1178552	-0.11	17344	0
6p0wt	HadGEM2-ES	Fixed imports	1187908	-0.10	17502	0
8p5wt	GFDL-ESM2M	Fixed imports	1223395	-0.07	16637	0
8p5wt	HadGEM2-ES	Fixed imports	1132023	-0.14	16921	0
8p5wt	IPSL-CM5A-LR	Fixed imports	1214310	-0.08	16295	0
8p5wt	MIROC	Fixed imports	1144187	-0.13	16166	0
8p5wt	NorESM1-M	Fixed imports	1174511	-0.11	16569	0
8p5wo	HadGEM2-ES	Fixed imports	1127856	-0.14	17178	0
NoCC	None	Facilitation + Tariff	5845726	3.44	65044	338724
2p6wt	HadGEM2-ES	Facilitation + Tariff	6266867	3.76	66401	380811
4p5wt	HadGEM2-ES	Facilitation + Tariff	5960152	3.52	67875	372203
6p0wt	HadGEM2-ES	Facilitation + Tariff	6167365	3.68	66789	393398
8p5wt	GFDL-ESM2M	Facilitation + Tariff	6473411	3.91	67580	340295
8p5wt	HadGEM2-ES	Facilitation + Tariff	5629993	3.27	69609	399729
8p5wt	IPSL-CM5A-LR	Facilitation + Tariff	5977386	3.54	70197	352002
8p5wt	MIROC	Facilitation + Tariff	5994512	3.55	65398	383632
8p5wt	NorESM1-M	Facilitation + Tariff	5745481	3.36	67255	392088
8p5wo	HadGEM2-ES	Facilitation + Tariff	5182680	2.93	18727	409417

GCM MIROC: MIROC-ESM-CHEM

Supplementary Table 3 | Global market responses to trade and climate change scenarios compared to the *Baseline trade* (T0) scenario by 2050.

RCP With / without CO_2	GCM	Trade scenario	Market responses			
			Global production efficiency, difference to T0 (%)	Crop calorie production, difference to T0 (%)	Food availability , difference to T0 (kcal/cap/day)	Agricultural prices, difference compared to T0 (%)
No CC	None	Fixed imports	0.00	0.00	-0.02	0.00
2p6wt	HadGEM2-ES	Fixed imports	0.00	-0.01	-3.15	0.01
4p5wt	HadGEM2-ES	Fixed imports	-0.01	-0.01	-7.59	0.02
6p0wt	HadGEM2-ES	Fixed imports	-0.01	-0.01	-9.19	0.02
8p5wt	GFDL-ESM2M	Fixed imports	-0.01	-0.01	-18.01	0.02
8p5wt	HadGEM2-ES	Fixed imports	-0.01	-0.02	-21.34	0.03
8p5wt	IPSL-CM5A-LR	Fixed imports	-0.02	-0.02	-21.73	0.04
8p5wt	MIROC	Fixed imports	-0.01	-0.01	-12.30	0.02
8p5wt	NorESM1-M	Fixed imports	-0.02	-0.02	-16.71	0.05
8p5wo	HadGEM2-ES	Fixed imports	-0.03	-0.03	-40.54	0.10
No CC	None	Facilitation + Tariff	0.08	0.08	78.96	-0.17
2p6wt	HadGEM2-ES	Facilitation + Tariff	0.07	0.08	82.80	-0.17
4p5wt	HadGEM2-ES	Facilitation + Tariff	0.07	0.08	73.93	-0.17
6p0wt	HadGEM2-ES	Facilitation + Tariff	0.07	0.08	75.67	-0.17
8p5wt	GFDL-ESM2M	Facilitation + Tariff	0.09	0.10	84.08	-0.18
8p5wt	HadGEM2-ES	Facilitation + Tariff	0.07	0.08	63.12	-0.16
8p5wt	IPSL-CM5A-LR	Facilitation + Tariff	0.05	0.08	65.44	-0.17
8p5wt	MIROC	Facilitation + Tariff	0.07	0.08	70.55	-0.17
8p5wt	NorESM1-M	Facilitation + Tariff	0.06	0.08	62.34	-0.16
8p5wo	HadGEM2-ES	Facilitation + Tariff	0.04	0.05	48.31	-0.15

GCM MIROC: MIROC-ESM-CHEM

Supplementary Table 4 | Results from OLS estimation of the impact of crop yields, trade costs and their interaction on population at risk of hunger and food availability including regional interaction effects. Observations are GLOBIOM output for 9 regions (EUR and CAN excluded) under the 5 different trade scenarios and 10 different climate change scenarios in 2050. The regression models are fully described in the Supplementary Methods.

		Food availability (kcal/cap/day)			Population at risk of hunger (million)		
		coefficient	*se*		*coefficient*	*se*	
Crop yield (% change)	CSI	144.38	*75.23*	*	-0.98	*0.49*	**
Crop yield (% change)	EAS	315.53	*64.28*	***	-18.93	*6.14*	***
Crop yield (% change)	LAC	286.44	*52.38*	***	-8.52	*1.23*	***
Crop yield (% change)	MNA	94.27	*80.54*		-0.95	*3.76*	
Crop yield (% change)	OCE	66.86	*101.28*		-0.04	*0.12*	
Crop yield (% change)	SAS	429.02	*53.89*	***	-78.95	*18.33*	***
Crop yield (% change)	SEA	312.61	*126.01*	**	-12.51	*6.88*	*
Crop yield (% change)	SSA	614.15	*106.97*	***	-92.60	*20.72*	***
Crop yield (% change)	USA	268.76	*34.80*	***	-0.14	*0.02*	***
Trade cost	CSI	-47.51	*10.78*	***	0.30	*0.05*	***
Trade cost	EAS	-37.11	*3.95*	***	2.61	*0.42*	***
Trade cost	LAC	-31.18	*6.19*	***	1.71	*0.21*	***
Trade cost	MNA	-75.09	*14.25*	***	4.31	*0.69*	***
Trade cost	OCE	35.05	*13.67*	**	-0.02	*0.02*	
Trade cost	SAS	-68.10	*6.51*	***	11.87	*1.25*	***
Trade cost	SEA	6.86	*14.40*		0.15	*0.84*	
Trade cost	SSA	-88.90	*8.93*	***	15.17	*1.67*	***
Trade cost	USA	32.50	*3.62*	***	-0.02	*0.00*	***
Crop yield (% change) x Trade cost	CSI	-41.83	*98.17*		0.14	*0.46*	
Crop yield (% change) x Trade cost	EAS	-89.27	*120.41*		10.14	*10.04*	
Crop yield (% change) x Trade cost	LAC	-111.99	*170.29*		3.84	*3.62*	
Crop yield (% change) x Trade cost	MNA	-135.55	*103.49*		7.51	*3.79*	**
Crop yield (% change) x Trade cost	OCE	115.82	*92.49*		-0.10	*0.10*	*
Crop yield (% change) x Trade cost	SAS	4.90	*71.44*		-33.03	*18.35*	*
Crop yield (% change) x Trade cost	SEA	41.41	*201.15*		0.76	*8.64*	
Crop yield (% change) x Trade cost	SSA	163.72	*149.63*		-60.40	*17.33*	***
Crop yield (% change) x Trade cost	USA	115.70	*35.32*	***	-0.07	*0.02*	***

Significance levels: $^{*}p<0.1$; $^{**}p<0.05$; $^{***}p<0.01$. Heteroskedastic robust standard errors. EUR and CAN are not included as they have always zero hunger. One outlier is removed: [CSI, T1, 8p5wo]. N = 449. Adjusted R squared is 0.999 for food availability regression and 0.982 for hunger regression.

Supplementary Table 5 | Regions, sub-regions and countries in GLOBIOM.

Region	Sub-region	Country
CAN	Canada	Canada
CSI	Former USSR	Belarus, Moldova, Ukraine, Russia, Azerbaidjan, Kazakhstan, Turkmenistan, Uzbekistan, Armenia, Georgia, Kyrgyzstan, Tajikistan
EAS	China	People's Republic of China, Hong Kong
	Japan	Japan
	South Korea	Korea
EUR	EU Baltic	Estonia, Latvia, Lithuania
	EU Central East	Bulgaria, Czech Republic, Hungary, Poland, Romania, Slovakia, Slovenia
	EU Mid West	Austria, Belgium, France, Germany, Luxembourg, Netherlands
	EU North	Denmark, Finland, Ireland, Sweden, United Kingdom
	EU South	Cyprus, Greece, Italy, Malta, Portugal, Spain
	Rest of Central Eastern Europe (RCEU)	Albania, Bosnia Herzegovina, Croatia, Macedonia, Serbia
	Rest of Western Europe (ROWE)	Iceland, Norway, Switzerland, Greenland
LAC	Brazil	Brazil
	Mexico	Mexico
	Central America (RCAM)	Bahamas, Belize, Costa Rica, Cuba, Dominican Republic, El Salvador, Guadeloupe, Guatemala, Jamaica, Nicaragua, Panama, Trinidad and Tobago
	South America (RSAM)	Argentina, Bolivia, Chile, Colombia, Ecuador,Guyana, Paraguay, Peru, Suriname, Uruguay, Venezuela
MNA	Middle East – North Africa	Egypt, Algeria, Libya, Morocco, Tunisia, Bahrain, Iran, Iraq, Israel, Jordan, Kuwait, Lebanon, Oman, Qatar, Saudi Arabia, Syria, United Arab Emirates, Yemen
	Turkey	Turkey
OCE	ANZ	Australia, New Zealand
	Pacific Islands	Fiji, French Polynesia, New Caledonia, Papua New Guinea, Samoa, Solomon Islands, Vanuatu
SAS	India	India
	Rest of South Asia (RSAS)	Afghanistan, Bangladesh, Bhutan, Nepal, Pakistan, Sri Lanka
SEA	South East Asia – other Pacific Asia (RSEA_OPA)	Brunei Daressalam, Indonesia, Malaysia, Myanmar, Philippines, Singapore, Thailand, East Timor
	South East Asia – (ex-)planned economies (RSEA_PAC)	Cambodia, DPR of Korea, Laos, Mongolia, Viet Nam
SSA	Congo Basin	Cameroon, Central African Republic, Congo Republic, Democratic Republic of Congo, Equatorial Guinea, Gabon
	Eastern Africa	Burundi, Ethiopia, Kenya, Tanzania, Uganda, Rwanda
	South Africa	South Africa
	Southern Africa	Angola, Botswana, Comoros, Lesotho, Madagascar, Malawi, Mauritius, Mozambique, Namibia, Reunion, Swaziland, Zambia, Zimbabwe
	Western Africa and Rest of Sub-Saharan Africa	Benin, Burkina Faso, Cape Verde, Chad, Côte d'Ivoire, Djibouti, Eritrea, Gambia, Ghana, Guinea, Guinea-Bissau, Liberia, Mali, Mauritania, Niger, Nigeria, Senegal, Sierra Leone, Somalia, Sudan, Togo
USA	USA Region	United States, Puerto Rico

Supplementary References

Bouët, A., Decreux, Y., Fontagné, L., Jean, S., & Laborde, D. (2008). Assessing applied protection across the world. *Review of International Economics*, *16*(5), 850–863. https://doi.org/10.1111/j.1467-9396.2008.00753.x

Hummels, D. (2001). *Toward a Geography of Trade Costs*.

Long, J. S., & Ervin, L. H. (2000). Using Heteroscedasticity Consistent Standard Errors in the Linear Regression Model. *The American Statistician*, *54*(3), 217–224.

McCarl, B. A., & Spreen, T. H. (2002). *Applied Mathematical Programming Using Algebraic Systems*. Texas A&M University 2011.